

First look at π^- asymmetries off CLAS12 RG-C longitudinally polarized ND_3 target

CLAS12 Collaboration Meeting
March 11, 2026

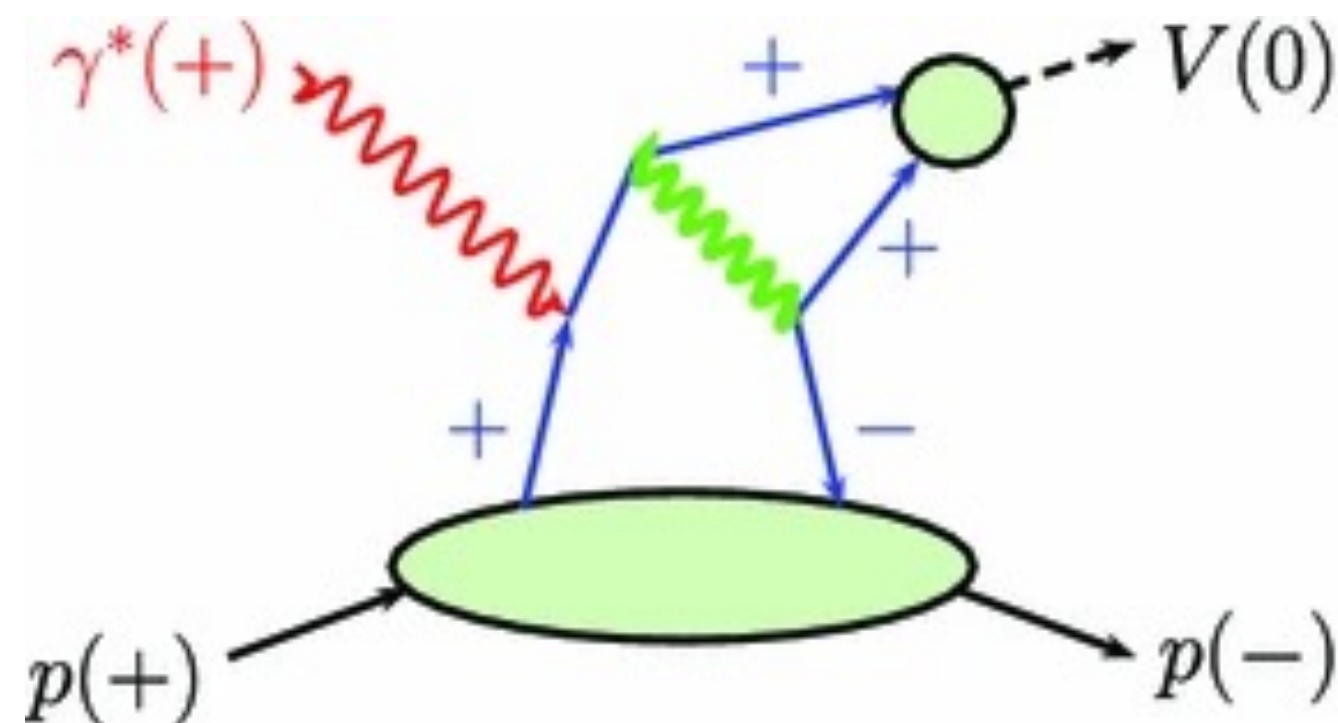
Maggie Kerr, Timothy Hayward, Harut Avakian



Overview: $DV\pi^-P, en \rightarrow ep\pi^-$

- Complementary to exclusive π^+ production analysis (see prev.)
 - Effects of nuclear target (Fermi motion)
 - First $DV\pi^-P$ BSA results from CLAS12
 - Potential new access to chiral odd GPDs of neutron from transversely polarized contributions
- Results still very preliminary!

$DV\pi^\pm P$ diagram



	U	L	T
U	\mathcal{H}		\mathcal{E}_T
L		$\tilde{\mathcal{H}}$	$\tilde{\mathcal{E}}_T$
T	\mathcal{E}	$\tilde{\mathcal{E}}$	$\mathcal{H}_T, \tilde{\mathcal{H}}_T$

chiral odd GPDs



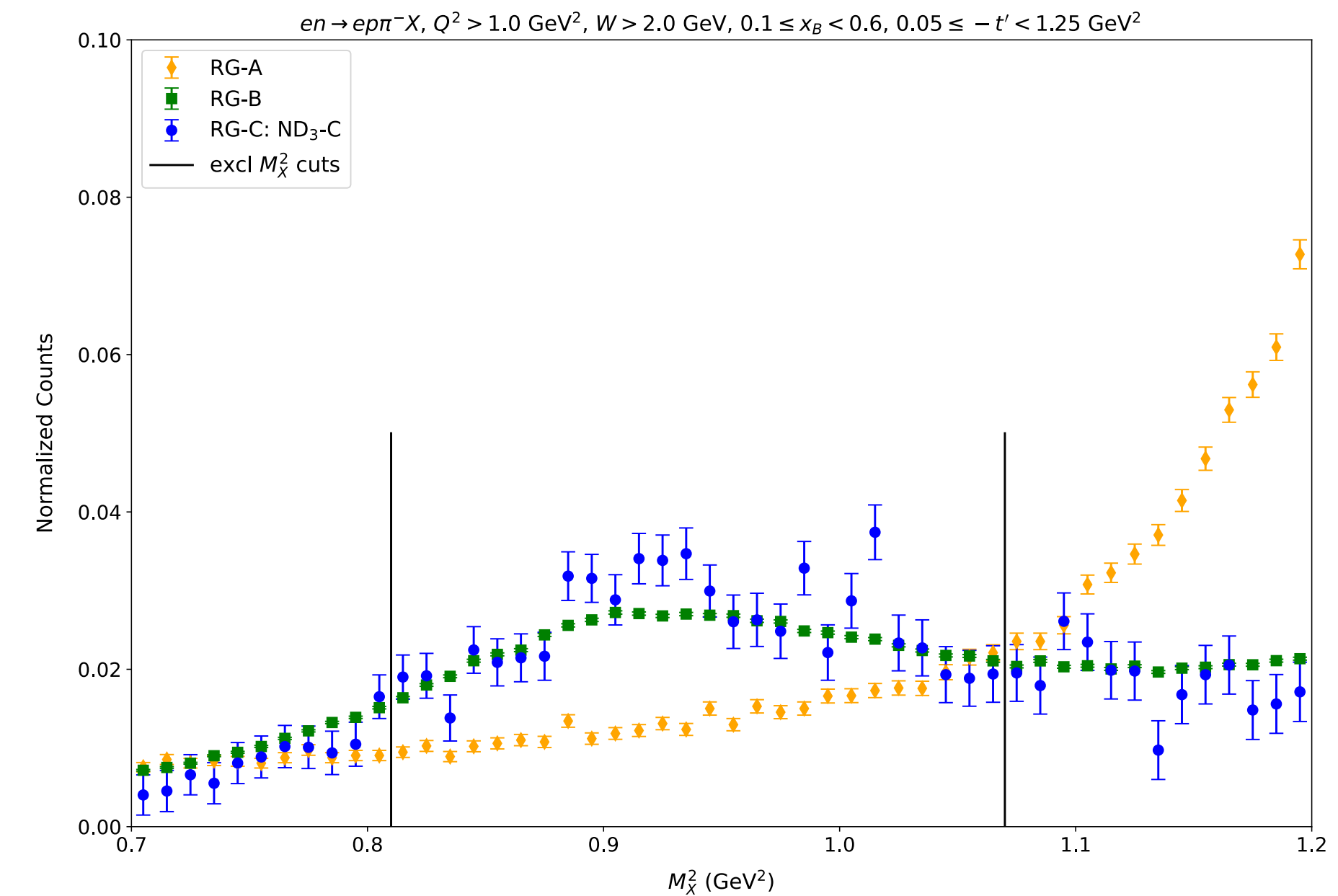
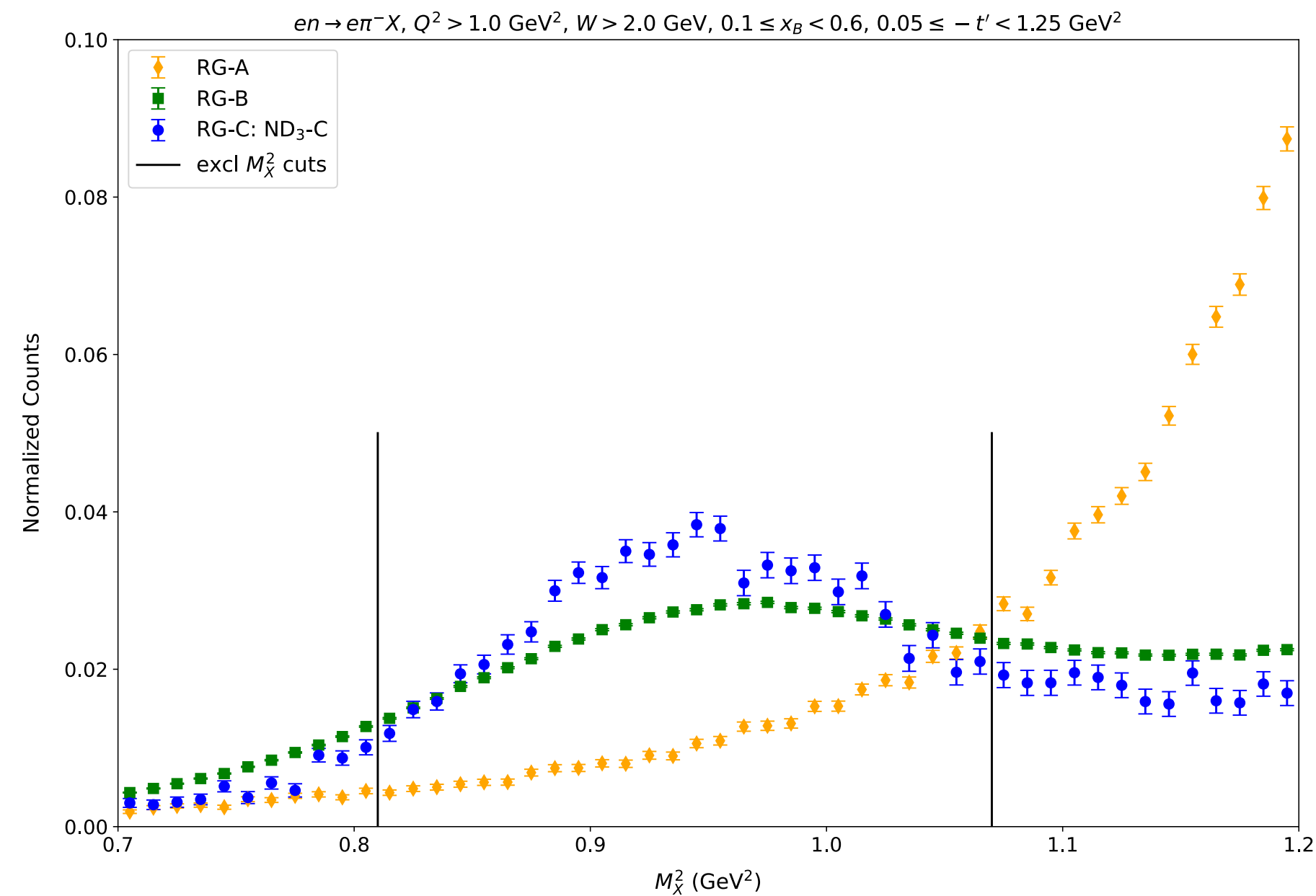
S. V. Goloskokov and P. Kroll, "Transversity in exclusive vector-meson leptonproduction," *Eur. Phys. J. C*, vol. 74, p. 2725, 2014.



Final state

$Q^2 > 1.0 \text{ GeV}^2$
 $W > 2.0 \text{ GeV}$
 $y < 0.75$
 $0.81 \text{ GeV}^2 < M_X^2 < 1.07 \text{ GeV}^2$

Two-dimensional binning to match π^+ analysis:
 $x_B \in [0.10, 0.25, 0.35, 0.45, 0.60)$
 $-t' \in [0.05, 0.25, 0.45, 0.65, 1.05, 1.25) \text{ GeV}^2$



$en \rightarrow e\pi^-X$: higher statistics, mirrors π^+ analysis,
 poorer resolution

$en \rightarrow ep\pi^-X$: lower statistics, cross-check with two
 particle final state, alternative methods for calculating
 kinematics



→ Subtracting “nuclear component” replicates RG-B
 M_X^2 peaks for both channels



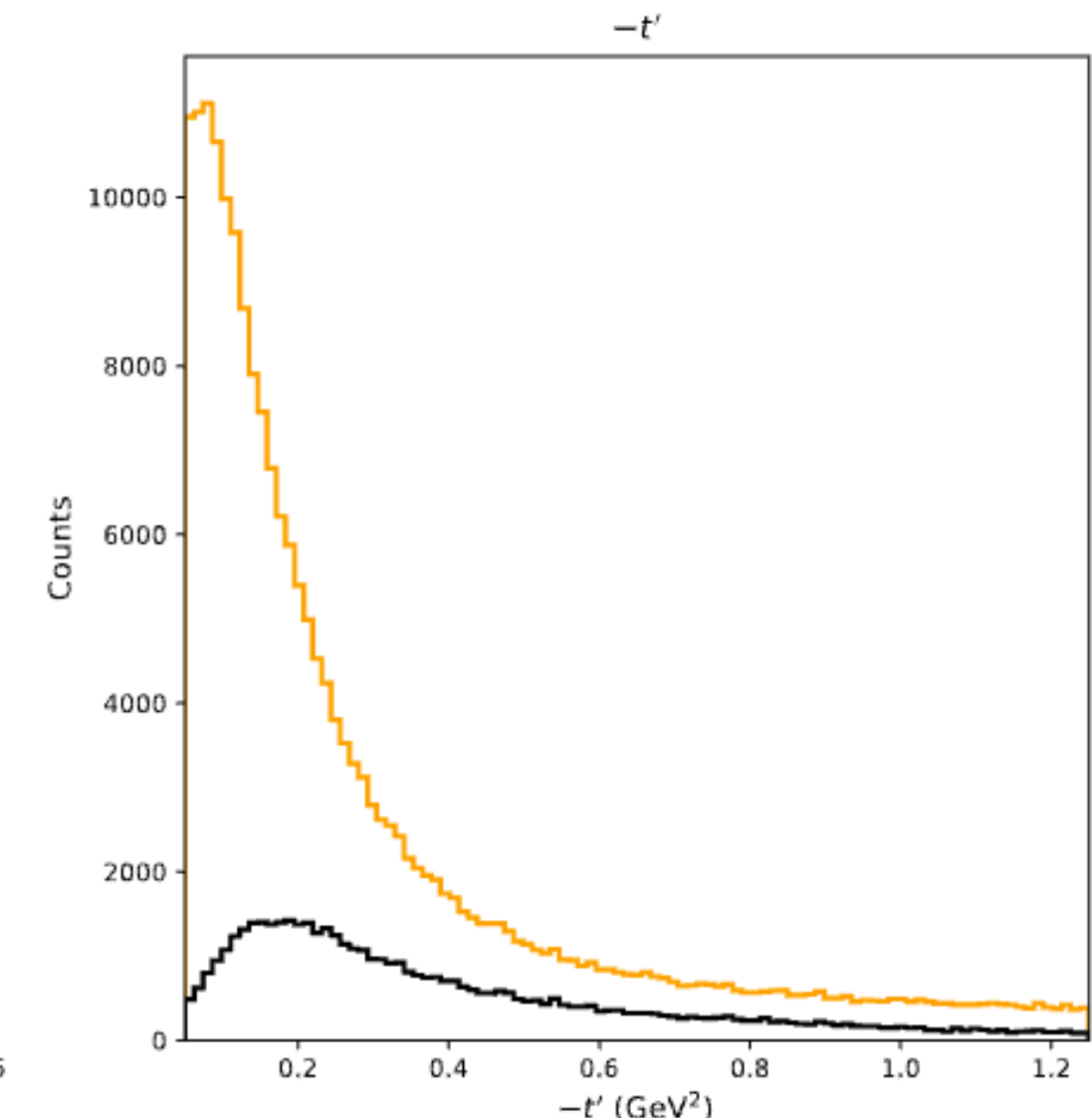
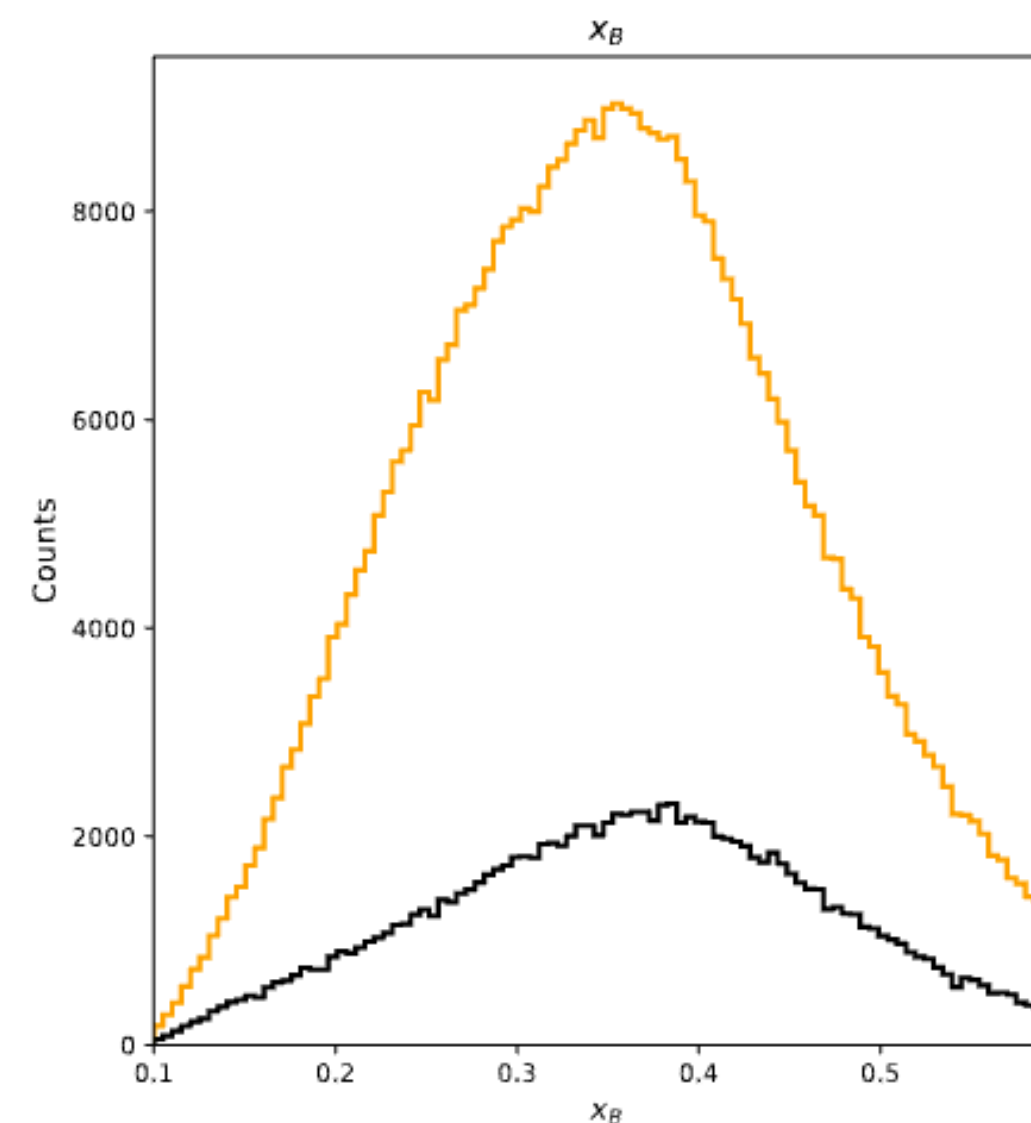
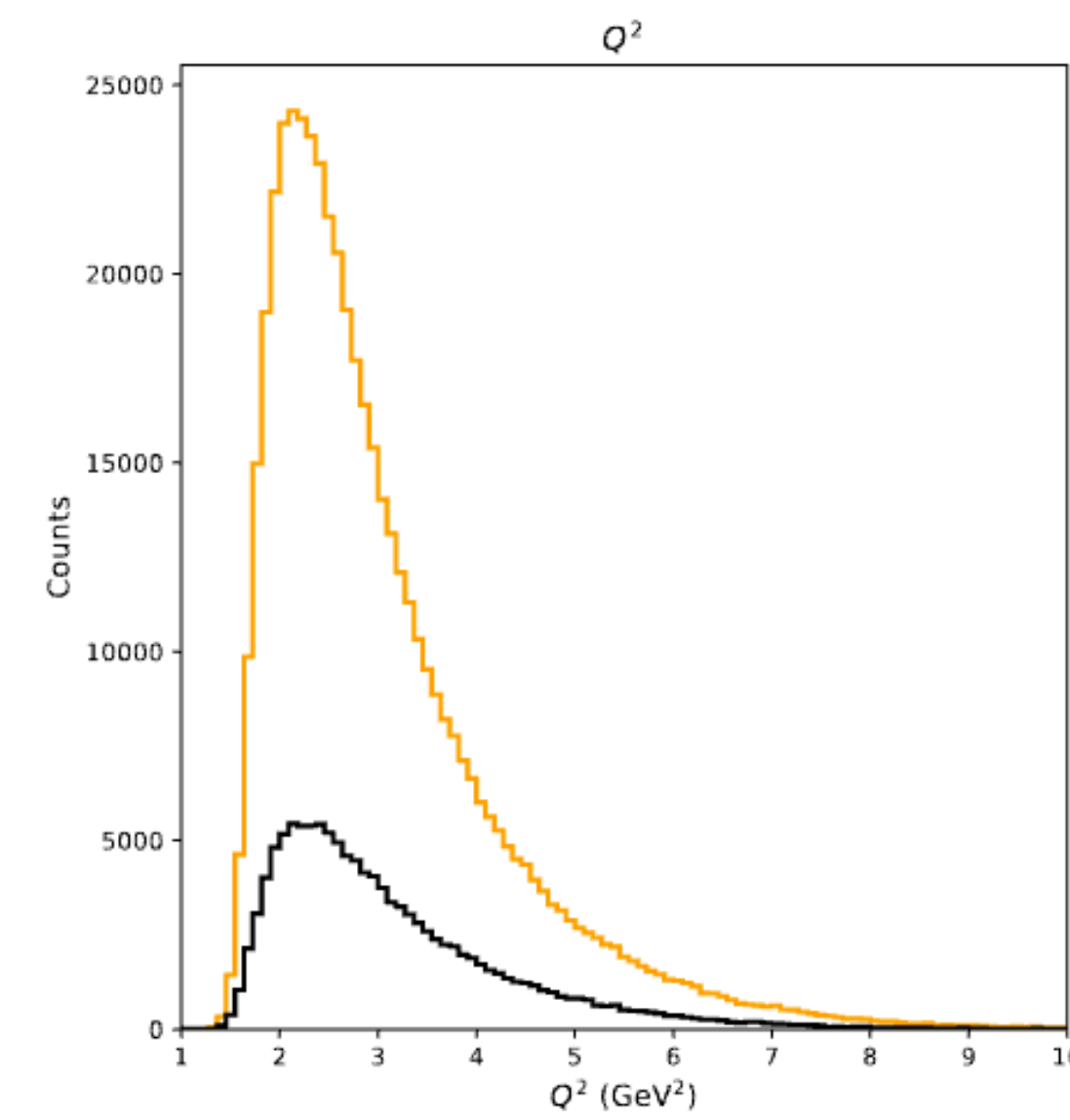
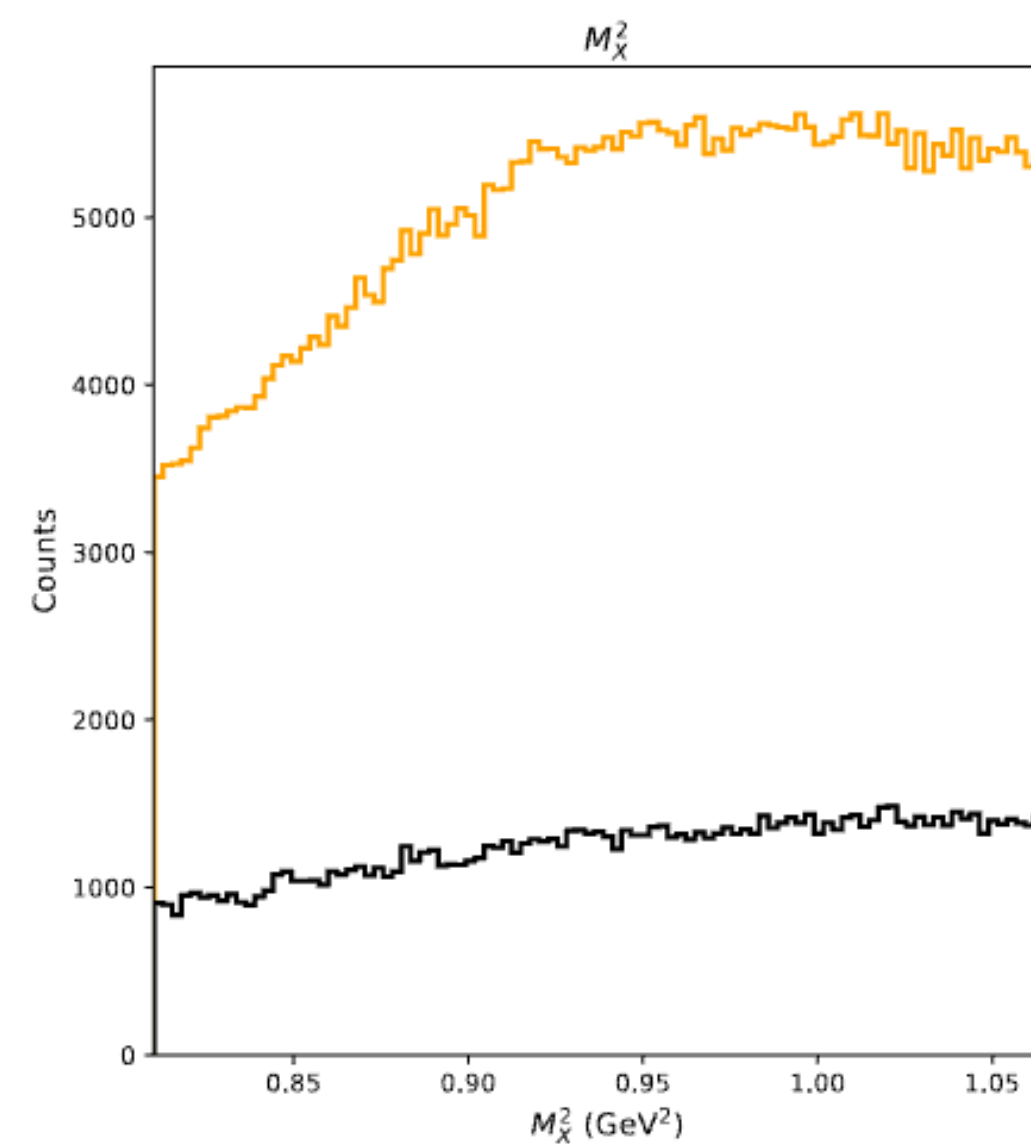
Comparing two and three particle final state yields

Yields for three particle final state ~25% of two particle final state count total

Multiple strategies to extract t :

- 1) $t = (p - p')^2$: sensitivity to Fermi motion
- 2) $t = (q - p_\pi)^2$: sensitivity to resolution effects, used for π^+ analysis, shown here

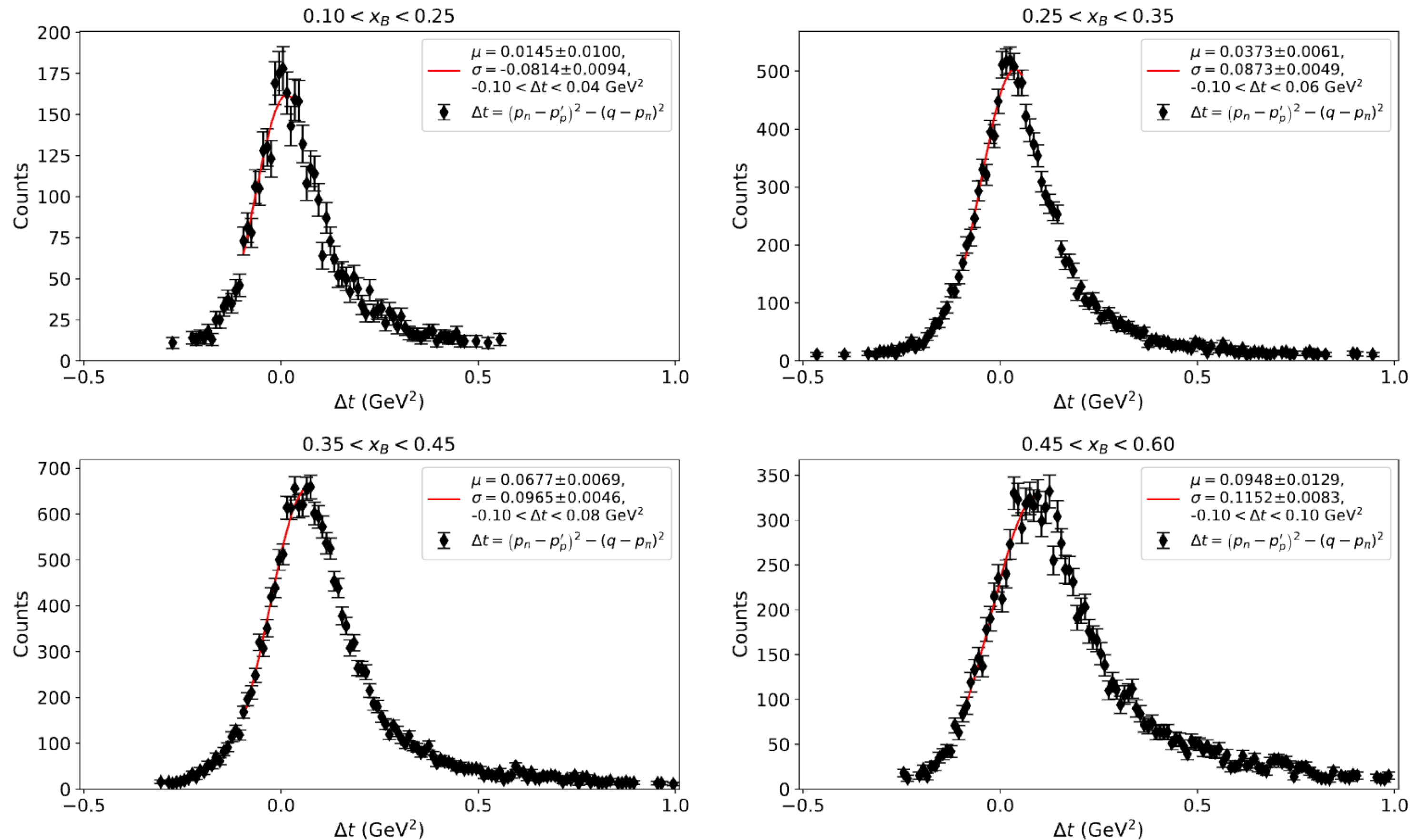
→ Similar kinematics with lower statistics in three particle final state



Alternate calculations for $-t \rightarrow -t'$

$$t' = t - t_{min}$$

$\Delta t = (p - p')^2 - (q - p_\pi)^2$ distributions for RG-C Fa22, on ND_3 (nuclear target with heightened Fermi motion)



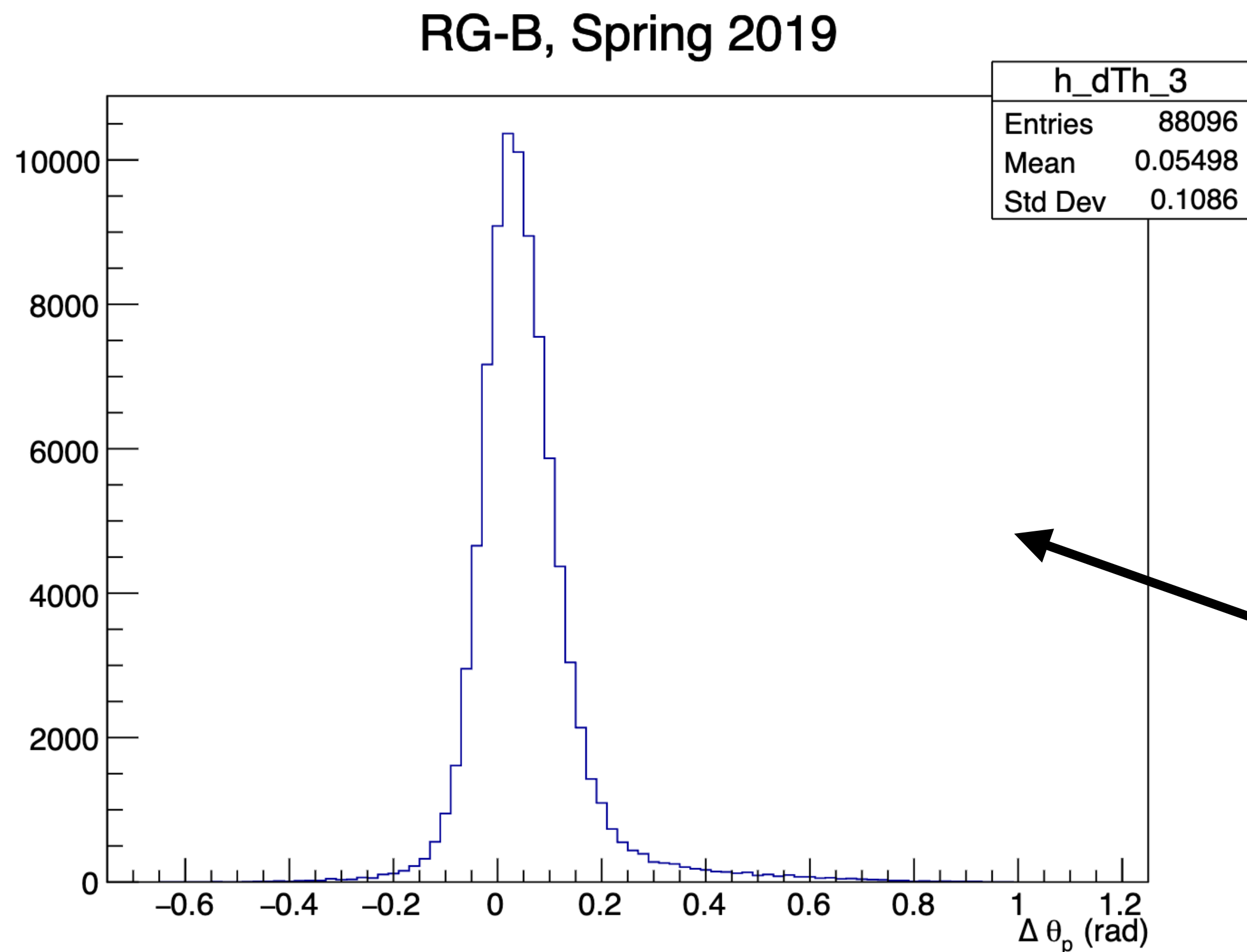
← width of distributions enhanced by Fermi motion, these are likely events occurring off nitrogen



→ How we use kinematics accessible with three particle final state to constrain Fermi motion?



Cone angle cut



- Measuring difference between detected and reconstructed (using π^- and e^-) proton θ
- When calculating proton 4-vector, we assume no Fermi motion
- Discrepancy provides insight on Fermi motion contributions
- Can use RG-B as baseline for expected distribution from deuterons (unpolarized LD_2 target)

RG-B Sp19
 $\mu = 0.05496$
 $\sigma = 0.1086$

vs.

RG-C
 $\mu \sim 0.24$
 $\sigma \sim 0.27$

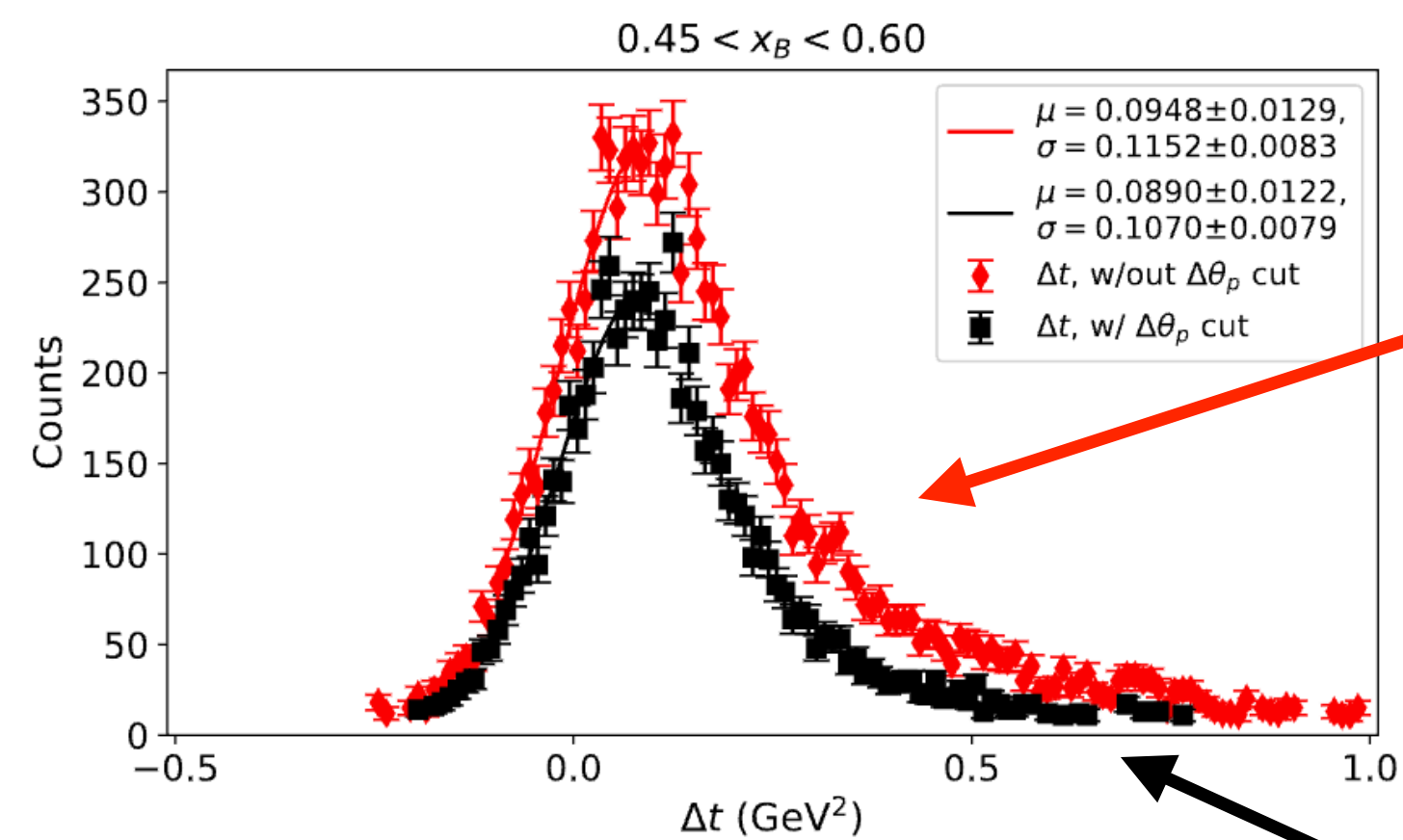
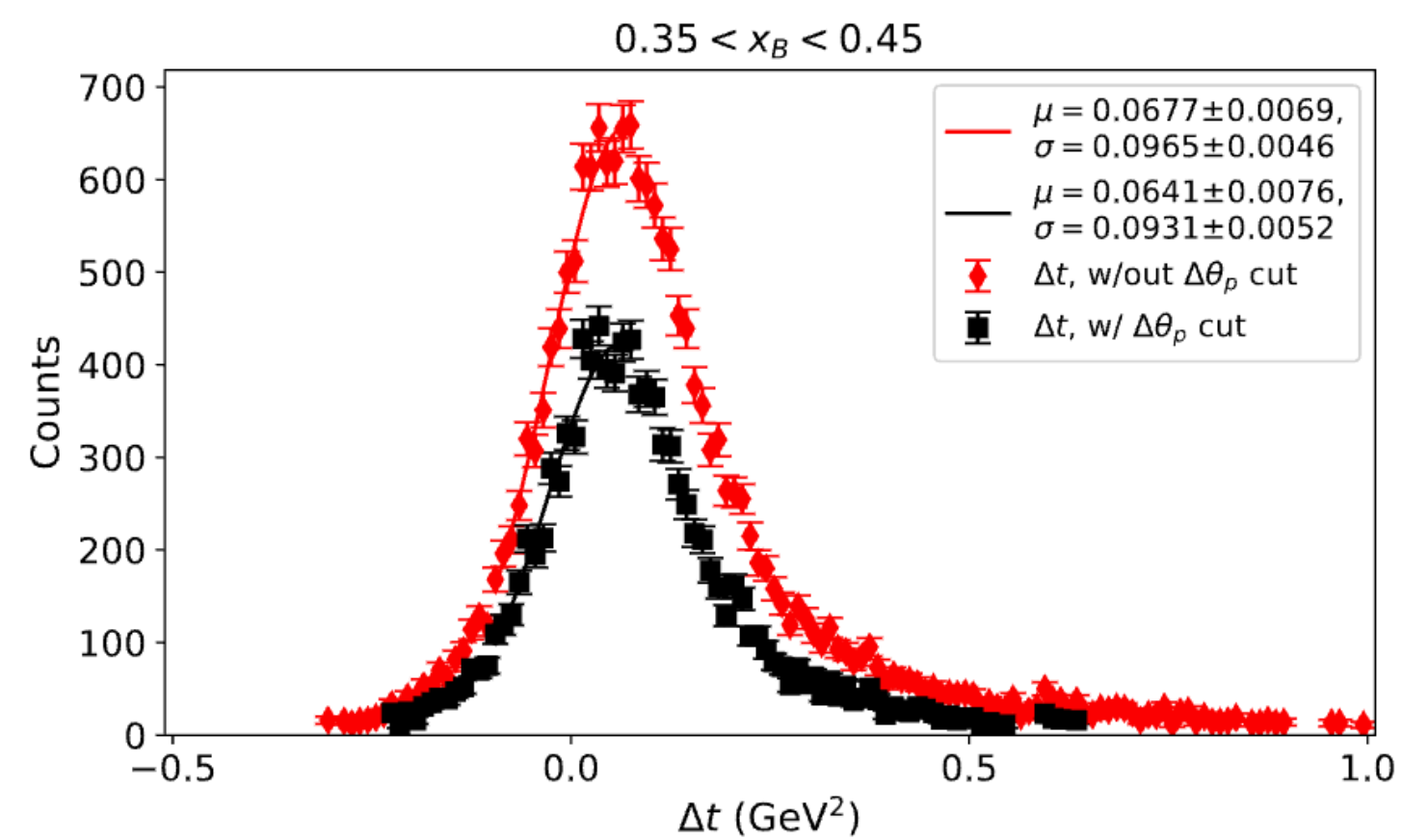
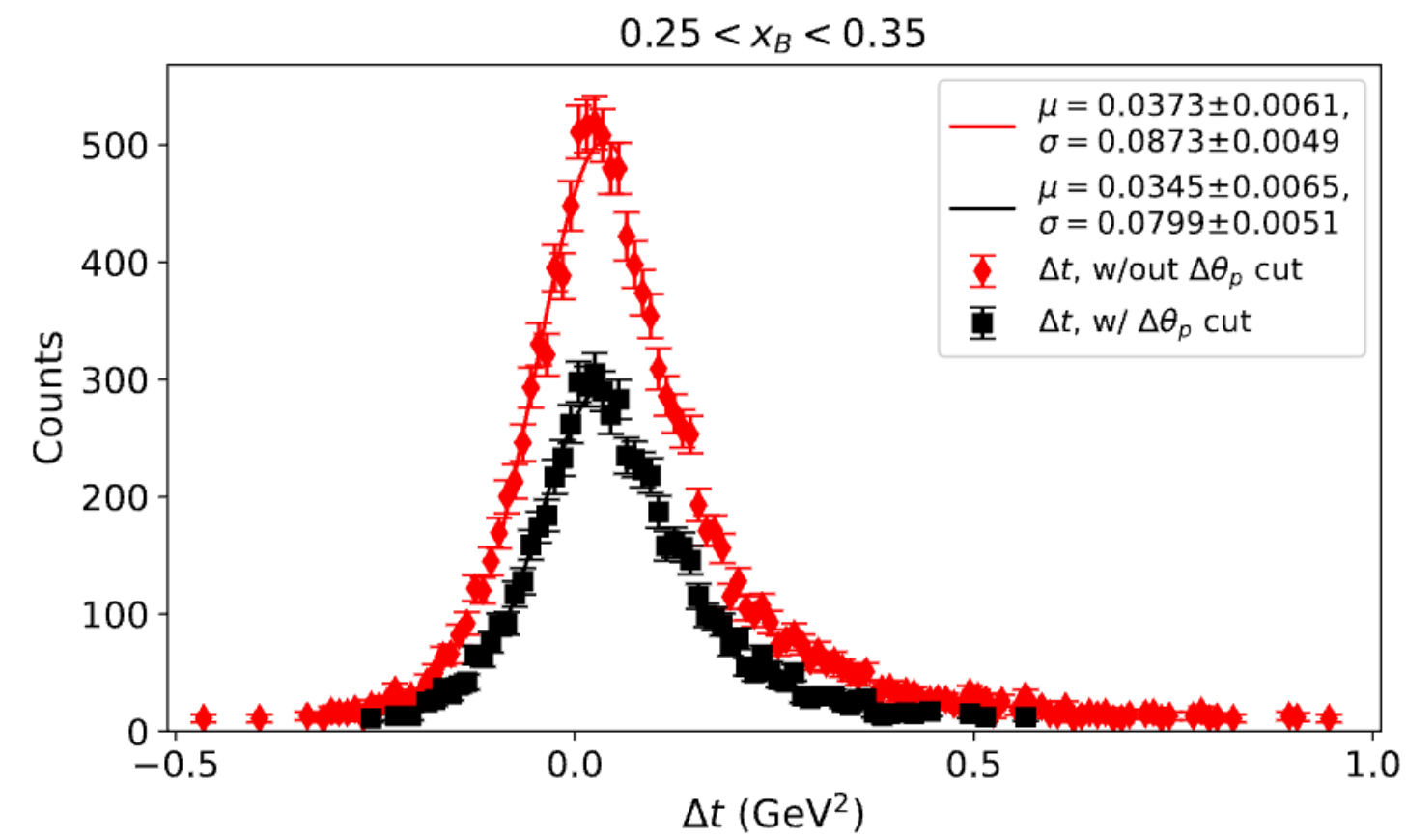
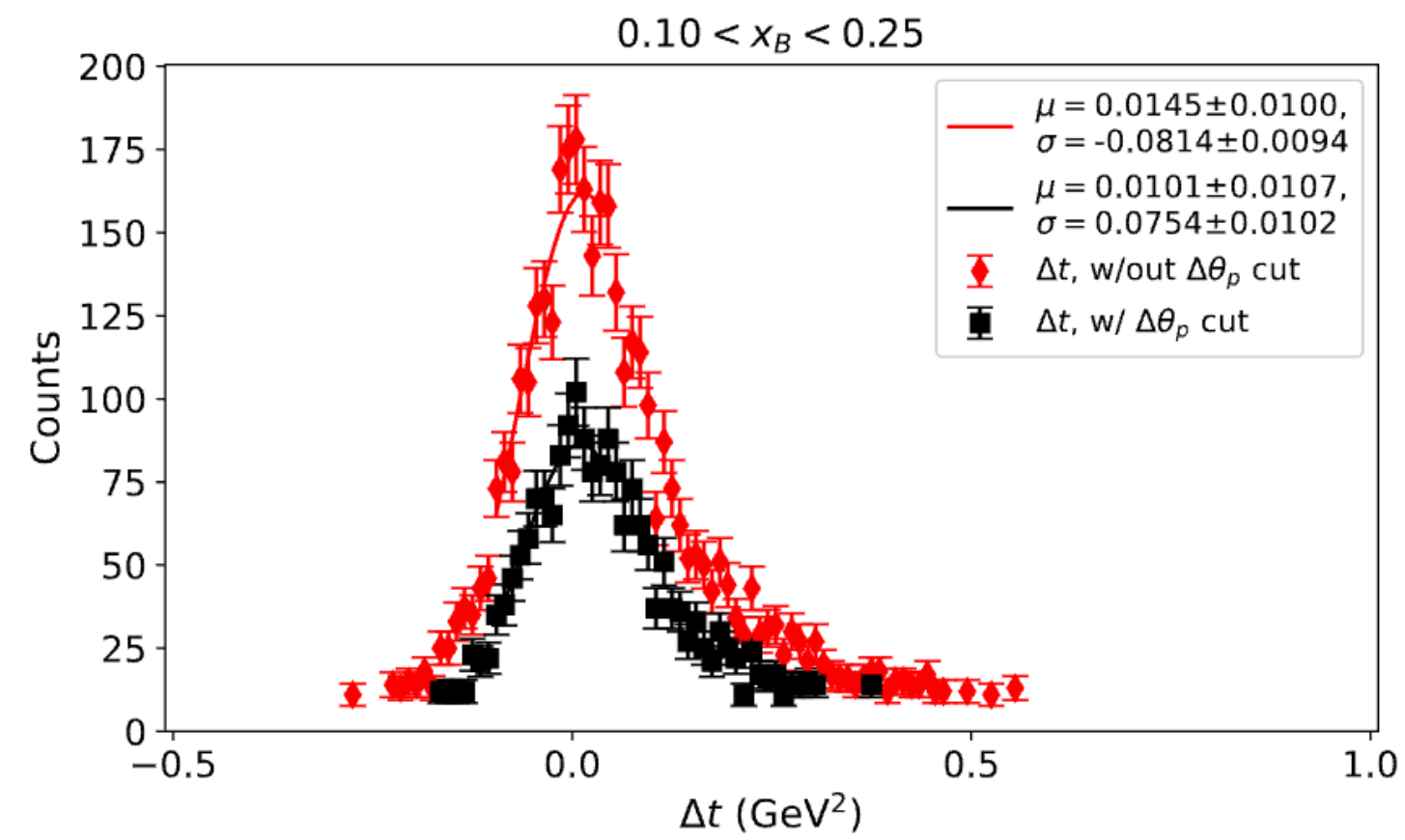


→ RG-B data helps us define a cone angle cut to select events off of deuterons for RG-C (RG-B $\mu \pm \sigma$)



Alternate calculations for $-t \rightarrow -t'$

$$t' = t - t_{min}$$



Constraining $\Delta\theta_p$ narrows Δt distribution, removing events identified as being nuclear in origin due to high Fermi motion

without $\Delta\theta_p$ cut

with $\Delta\theta_p$ cut



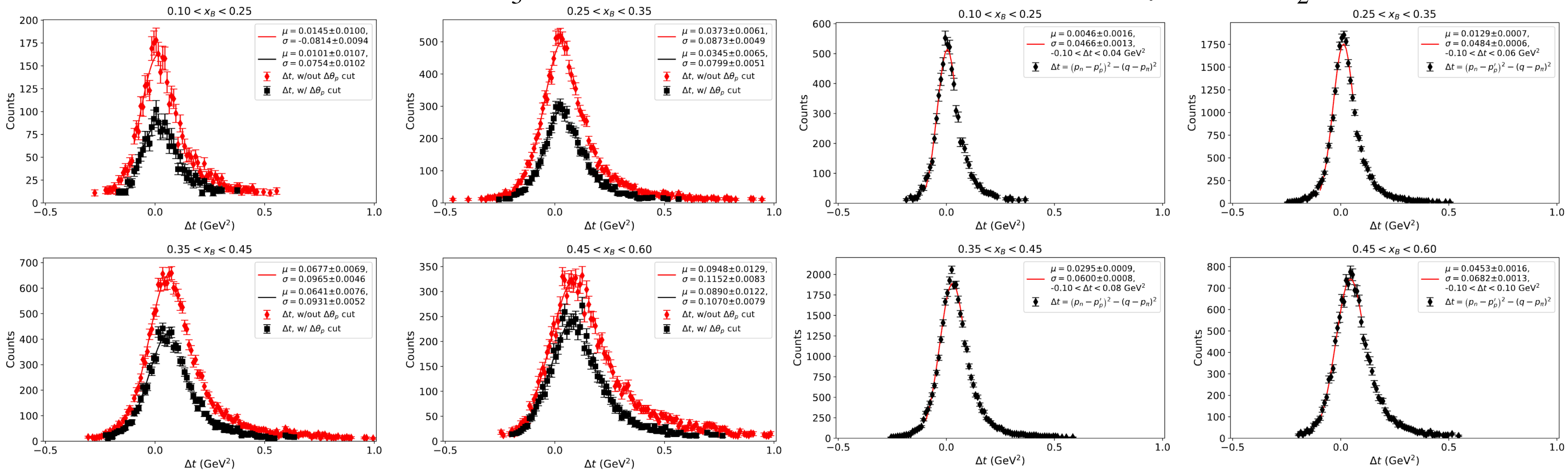
Alternate calculations for $-t \rightarrow -t'$

$$t' = t - t_{min}$$

Still not as narrow as RG-B Δt distributions!

RG-C Fa22, on ND_3

RG-B Sp19, on LD_2



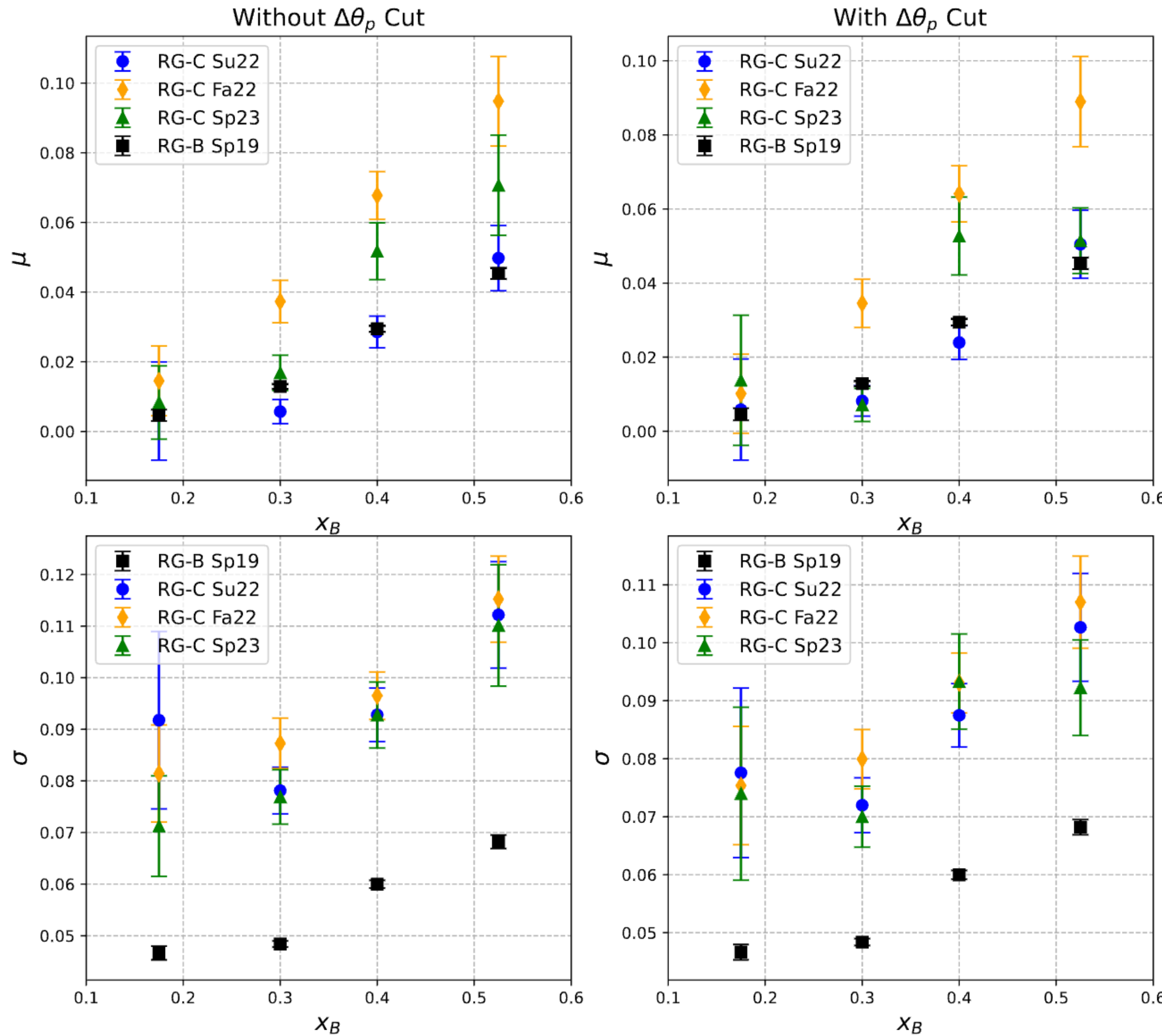
$\rightarrow \Delta\theta_p$ cuts removes some Fermi motion effects, but not all (other effects as well)



Alternate calculations for $-t \rightarrow -t'$

$$t' = t - t_{min}$$

Direct comparison using fits to Gaussian:



μ : resolution of “reconstructed” t ; relatively consistent (using same CLAS12 detectors)

σ : Fermi motion; clear differences between RG-B and RG-C, even with $\Delta\theta_p$ cut



Dilution factor and packing fraction

Dilution factor, packing fraction calculations and methodology by Sebastian Kuhn and Derek Holmberg

- Dilution factor scales results to reflect polarized components of target

$$DF = \frac{(n_A - n_{MT}) (n_{CD} - 0.757666n_C - 0.005200n_{MT} - 0.237132n_F)}{n_A (n_{CD} - 0.168370n_C - 0.865973n_{MT} + 0.03434n_F)}$$

where $n_X = \frac{N_X}{F_X^{CC}}$

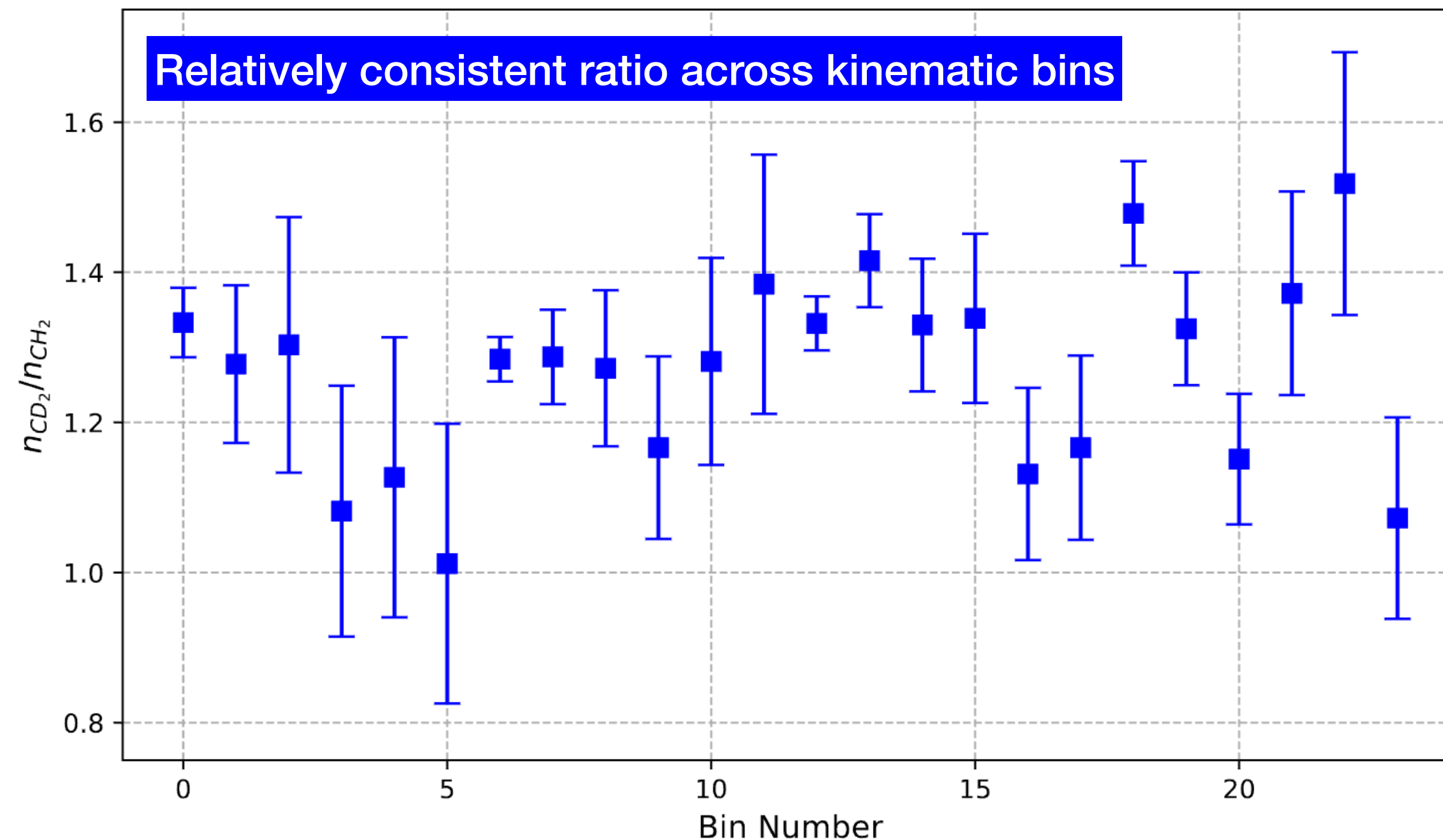
$$PF = 0.442453 \frac{n_A - n_{MT}}{n_{CD} - 0.168370n_C - 0.865973n_{MT} + 0.03434n_F}$$

- Measures of how tightly molecules are “packed” into the target cell
- Should be uniform across processes → useful for comparison
- Can also be used to construct dilution factor, yielding a near identical result with somewhat higher uncertainty



$CH_2 \rightarrow CD_2$ conversion technique

- Sp23 only RG-C run period with data off entire target set for dilution factor
 - Su22 & Fa22 missing data off of CD_2 target so manipulation required to calculate these dilution factors



1. Calculate charge-normalized counts per kinematic bin for Sp23 CH_2 and CD_2 targets
2. Construct ratio (per kinematic bin) of CH_2 to CD_2 using Sp23 data
3. Apply ratio to charge-normalized counts per kinematic bin of Su22, Fa22 CH_2 data



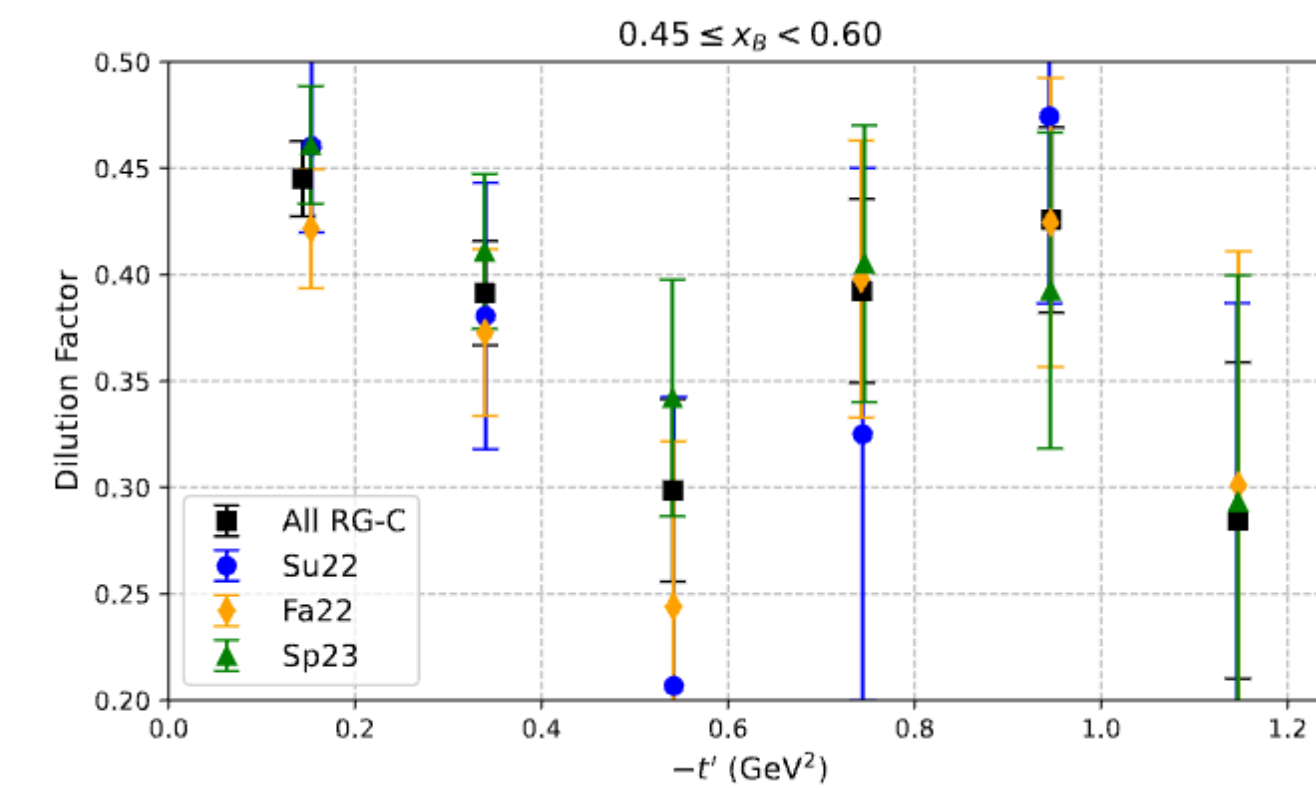
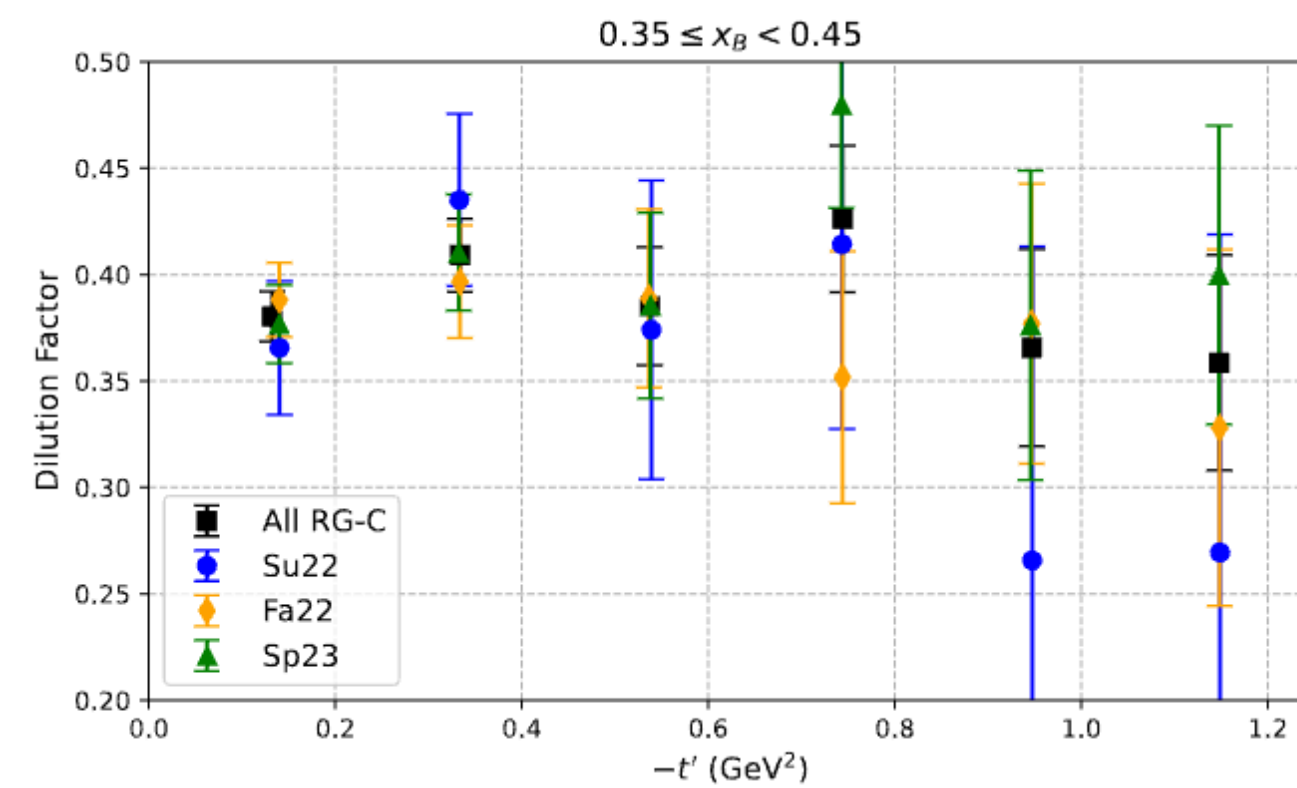
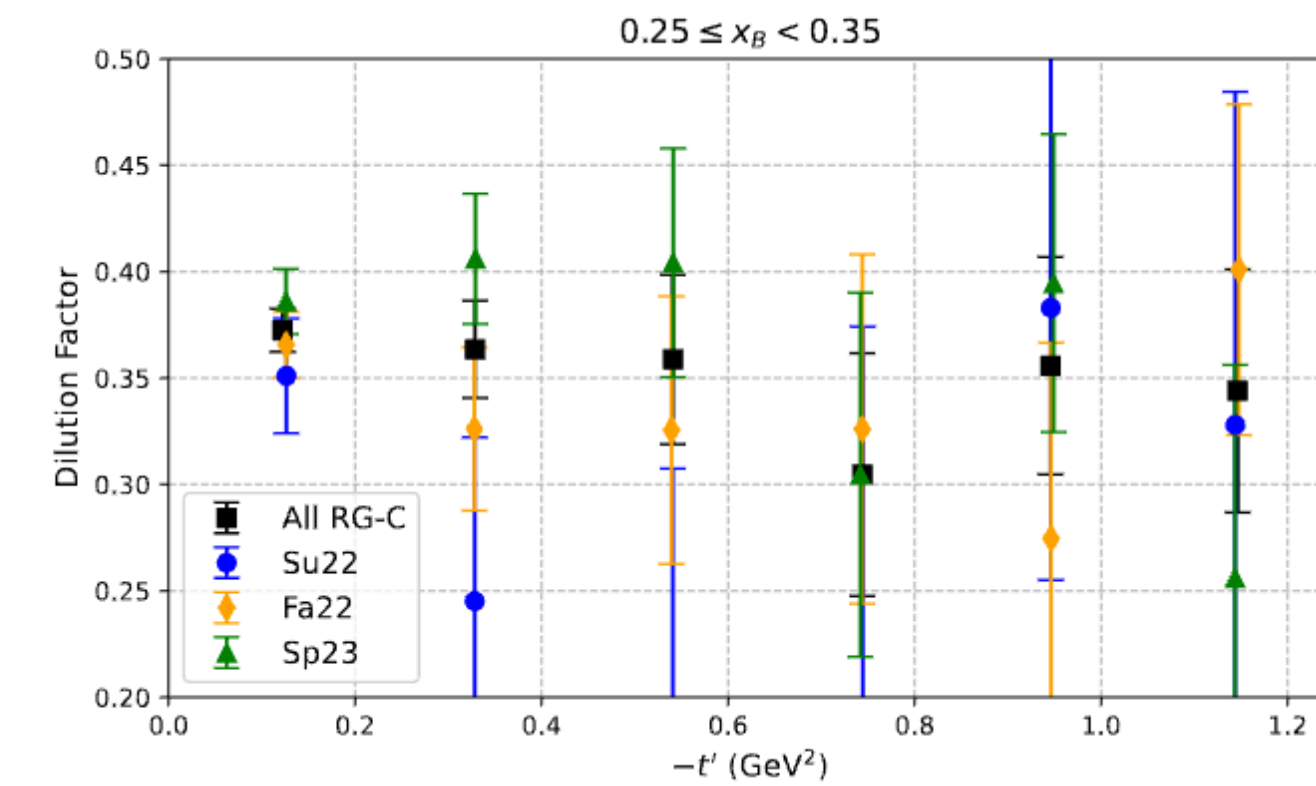
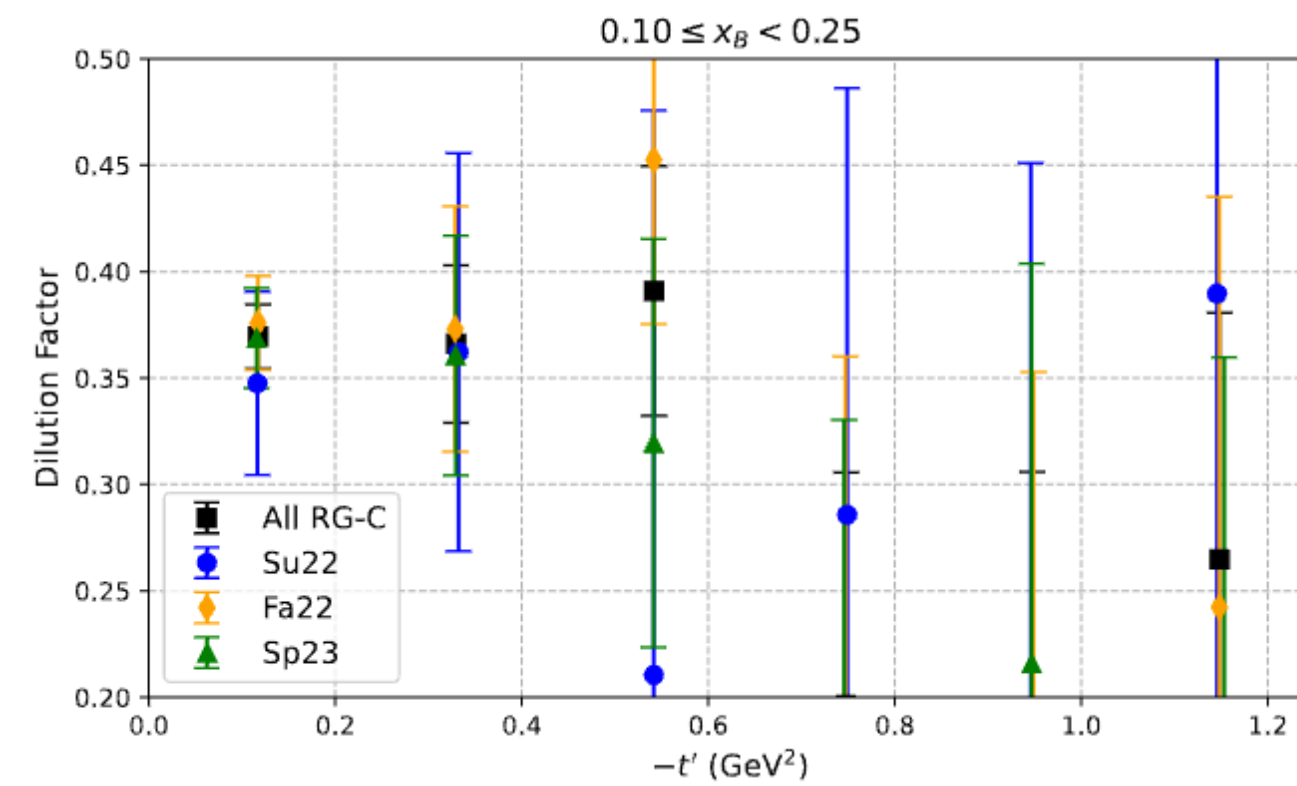
→ Despite missing CD_2 data in two periods, we can manipulate CH_2 data to still analyze full RG-C data set



Dilution factor studies

$$en \rightarrow e(p)\pi^-$$

Results over two-dimensional kinematic binning



Su22	Fa22	Sp23
0.372 ± 0.013	0.376 ± 0.010	0.391 ± 0.010



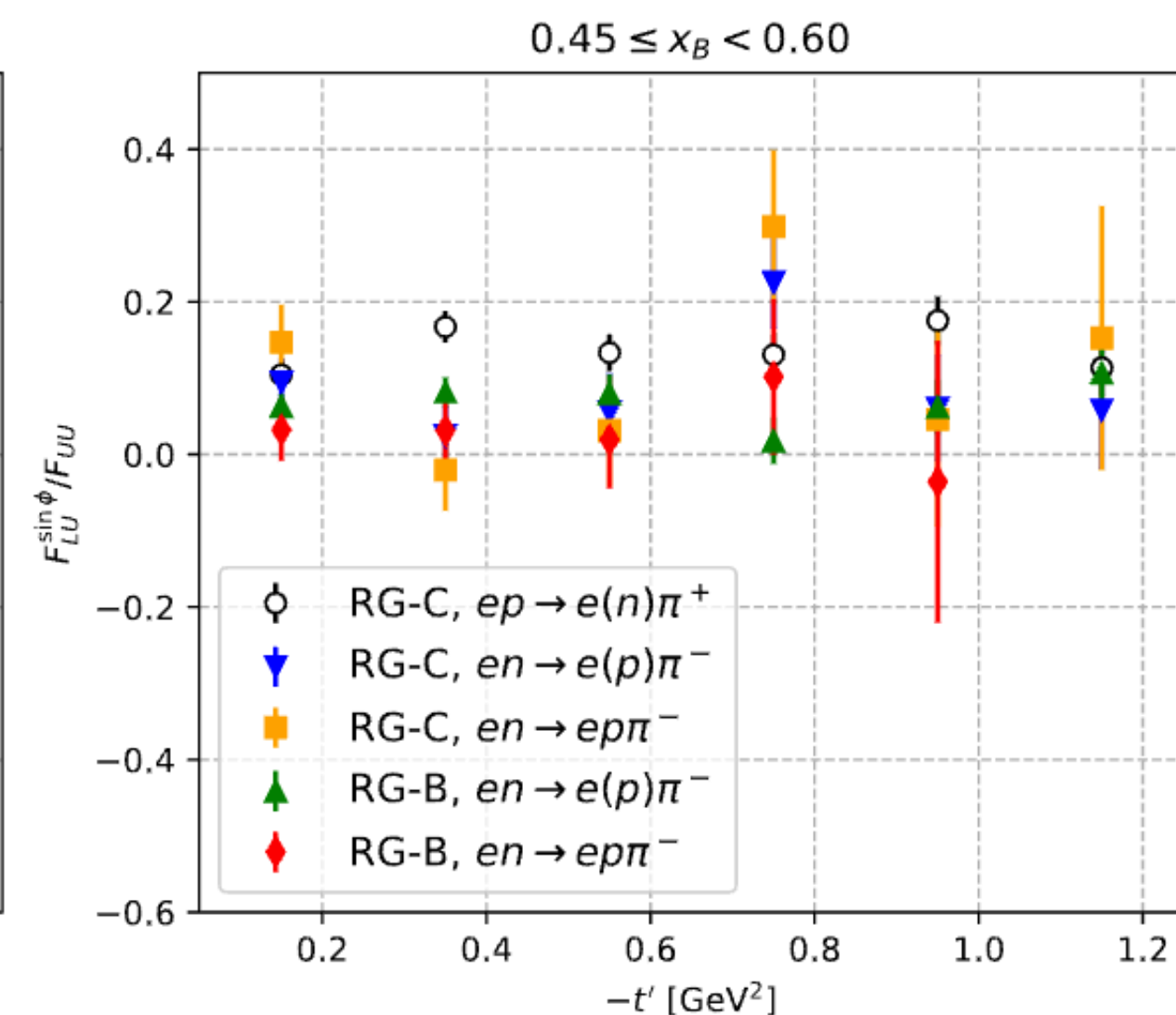
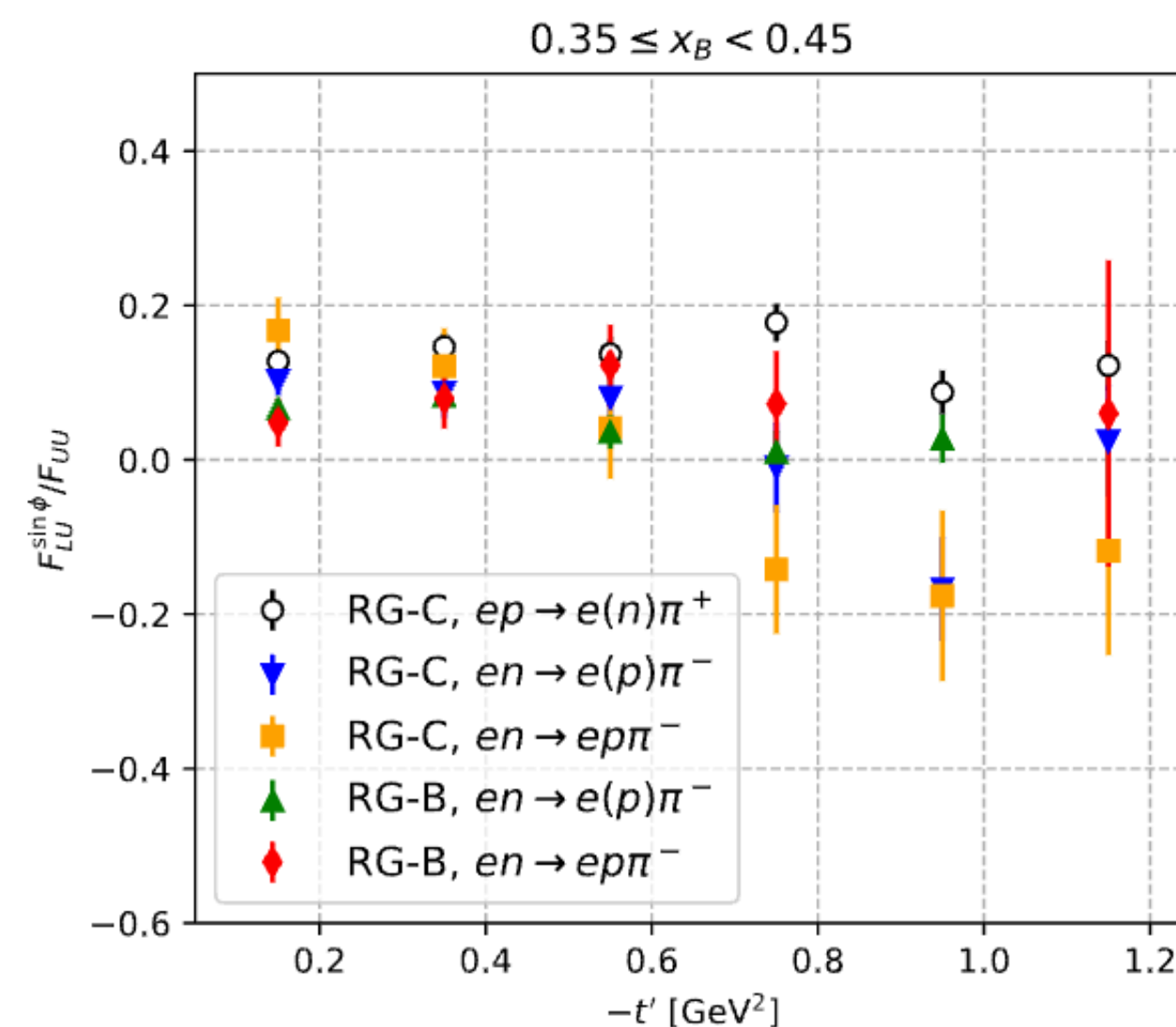
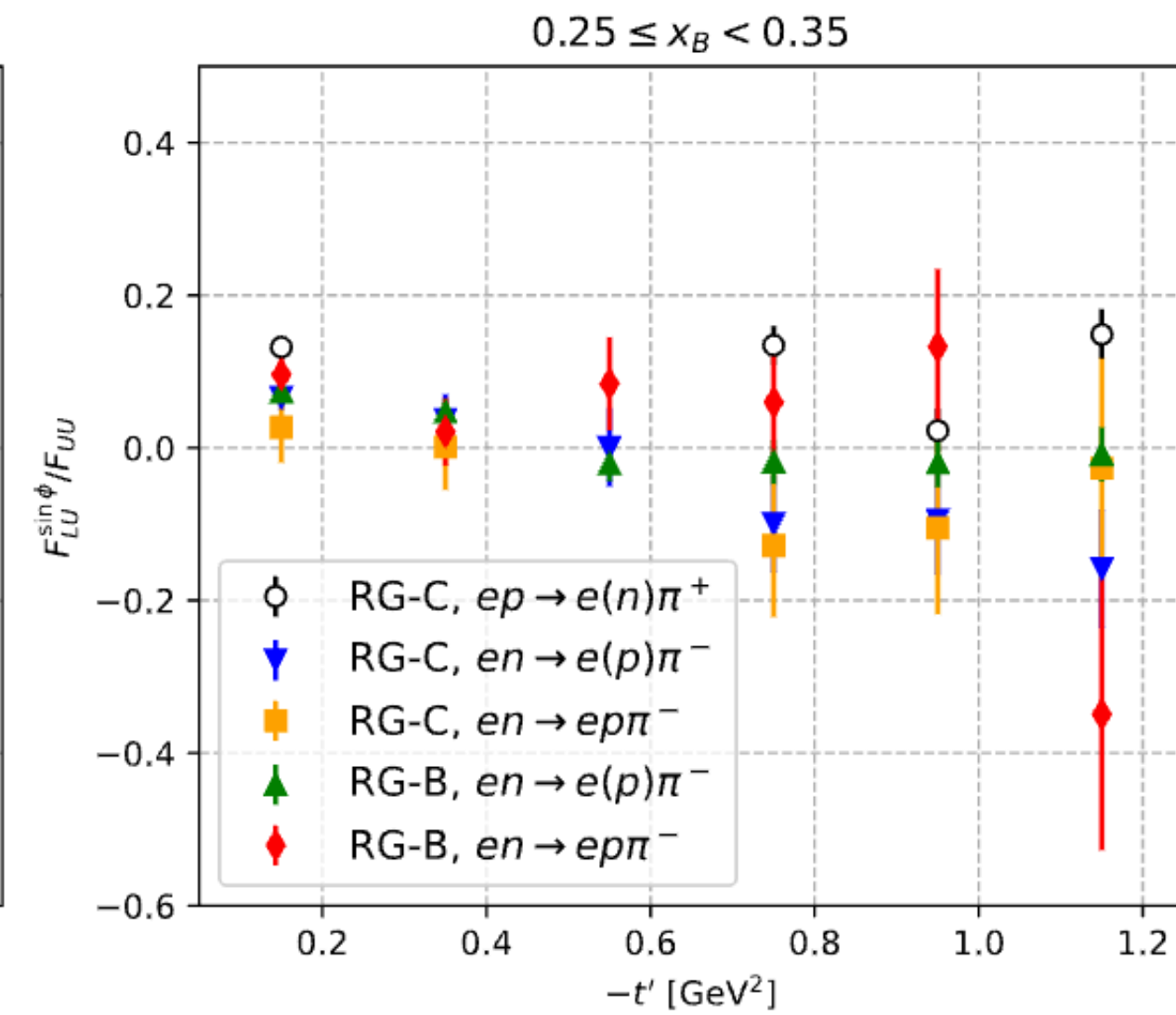
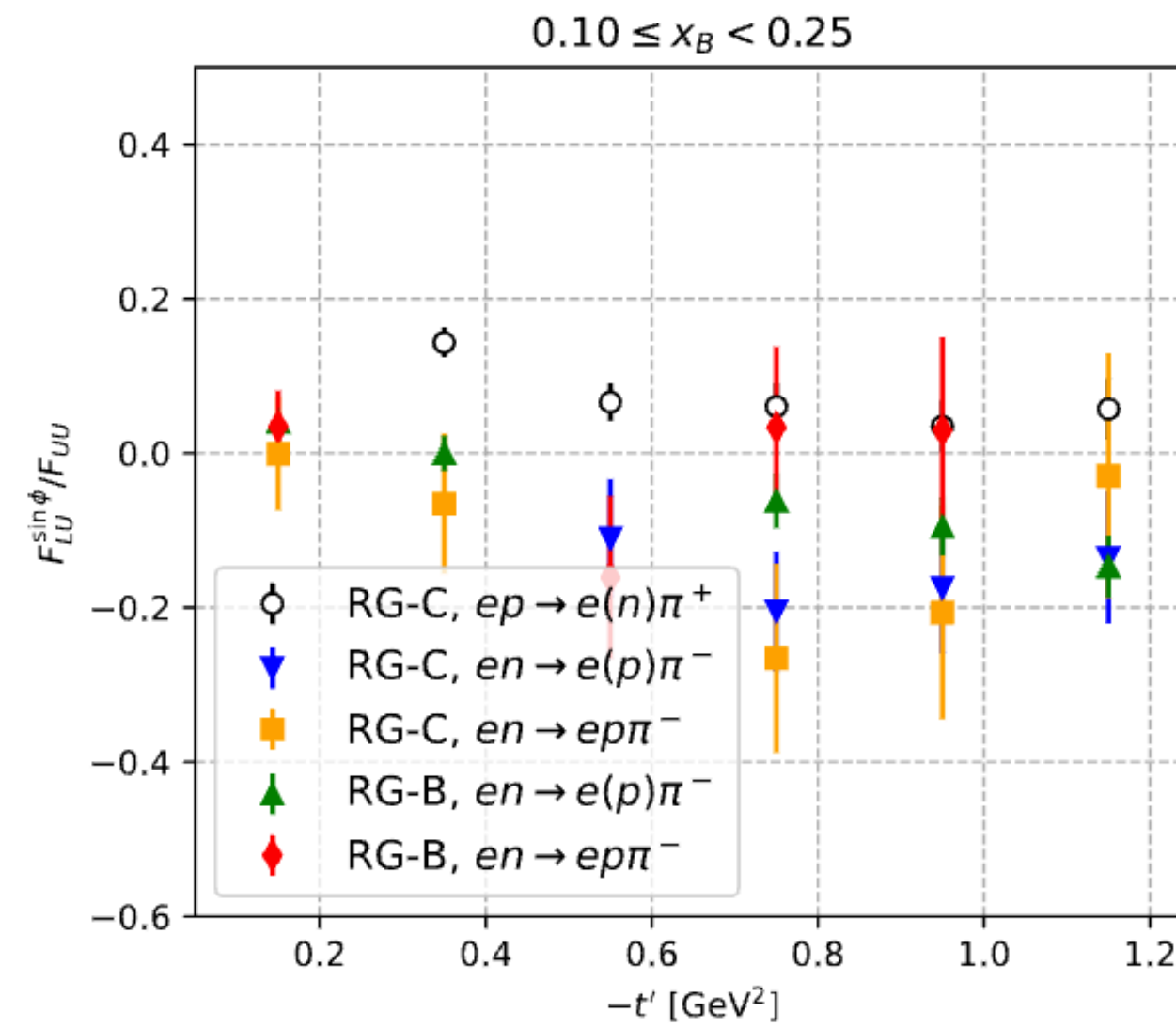
$A_{LU} \rightarrow F_{LU}^{\sin \phi} / F_{UU}$ results

$$A_{LU} = C_{LU} + \frac{\frac{W}{A} \frac{F_{LU}^{\sin \phi}}{F_{UU}} \sin \phi}{1 + \frac{V}{A} \frac{F_{UU}^{\cos \phi}}{F_{UU}} \cos \phi + \frac{B}{A} \frac{F_{UU}^{\cos 2\phi}}{F_{UU}} \cos 2\phi}$$

(denominator set to 1 for this study)

Comparing results from Fa22 RG-C π^+ , Fa22 RG-C, Sp19 RG-B π^- & $p\pi^-$

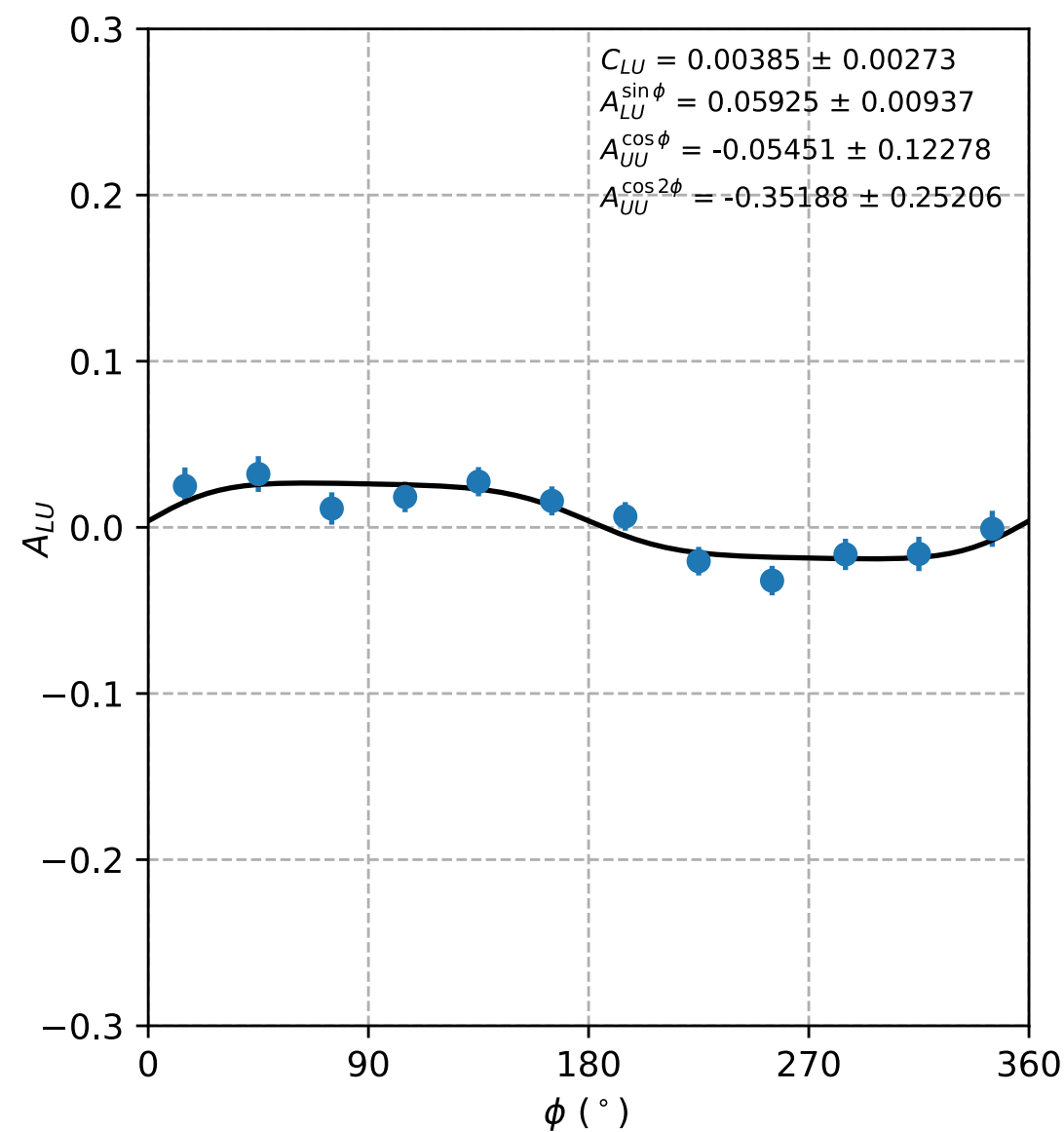
π^+ $F_{LU}^{\sin \phi} / F_{UU}$ amplitude fit possibly slightly larger than for $\pi^-/p\pi^-$ but run period $\pi^-/p\pi^-$ are overall consistent



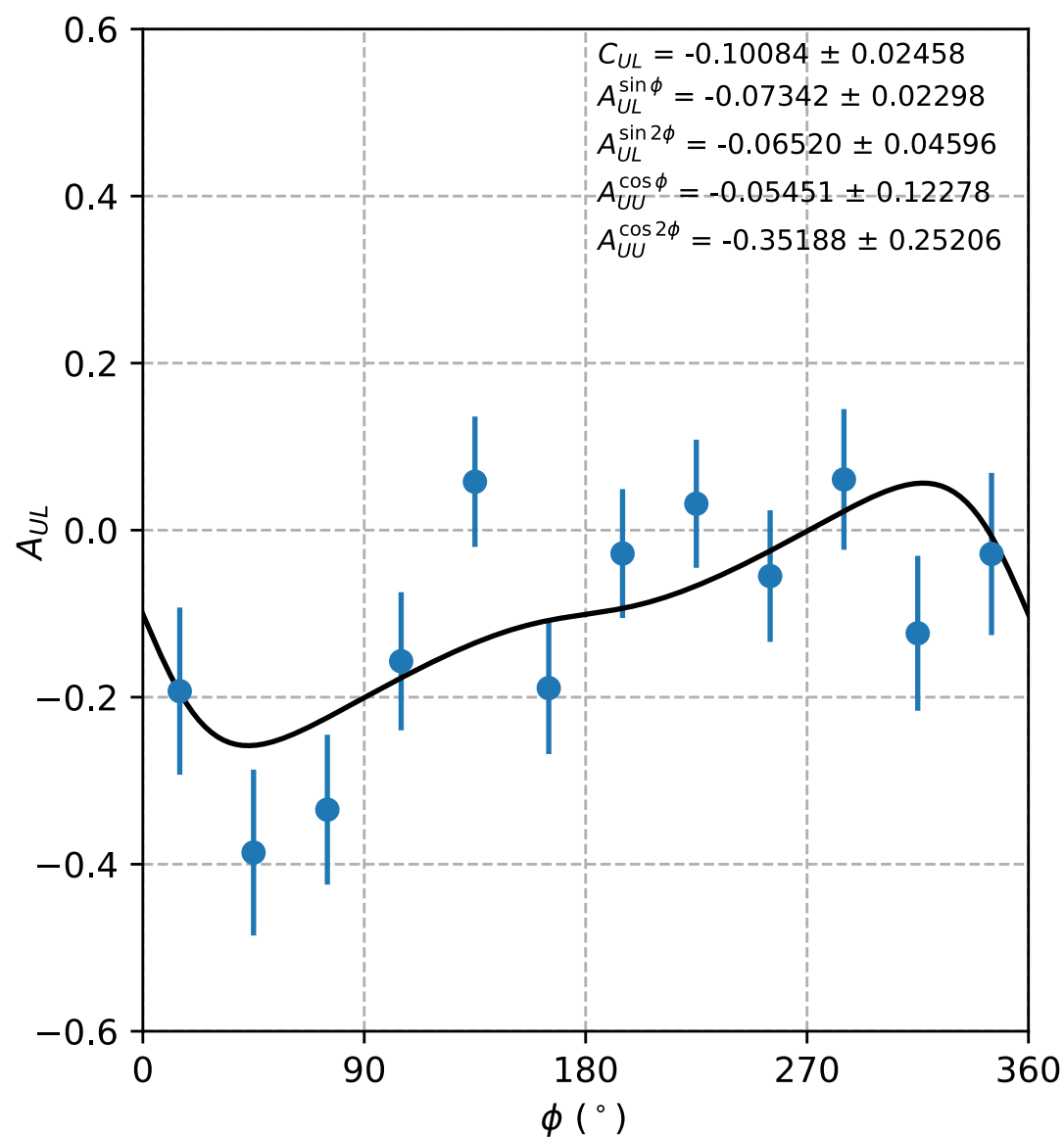
Preliminary spin asymmetry set results

Integrated results for Fall 2022

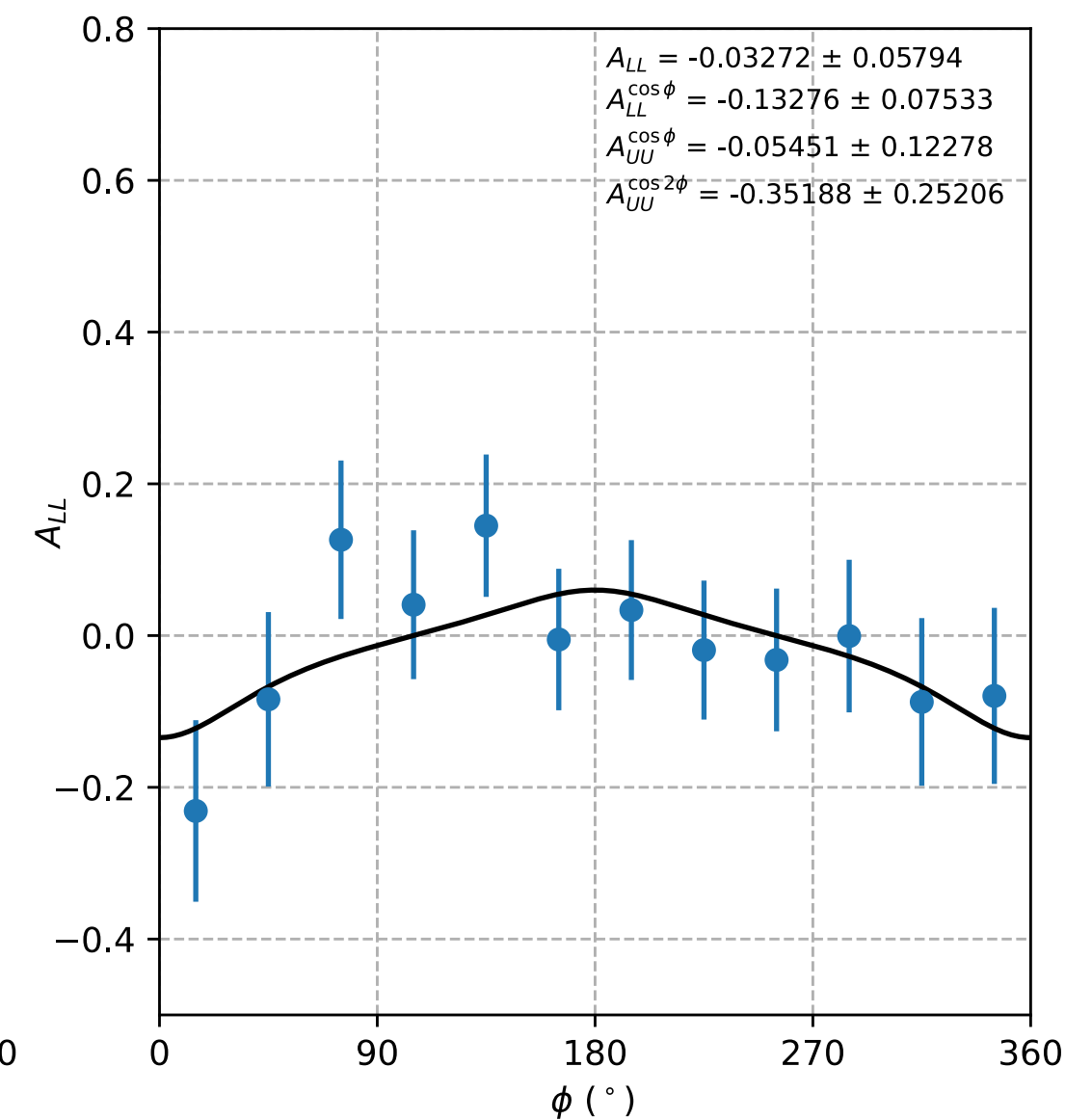
A_{LU}



A_{UL}



A_{LL}



BSA
looks as
expected



Difficult to
comment
on DSA
until issues
with TSA
resolved



- 1) TSA C_{UL} should be consistent with zero if charge normalized counts are accurate
 $\rightarrow \sim 4\sigma$ deviation in Fall22, also difficulties in other run periods with inconsistent offsets and distribution shapes for TSA

- Working with RG-C collaborators to identify potential runs with issues



- 2) Preliminary observations for TSA shape \rightarrow possible non-zero $\sin 2\phi$ modulations for $DV\pi^-P$ (as seen in $DV\pi^+P$)



Summary and outlook

- ✓ RG-C $DV\pi^-P$ channel complementary to $DV\pi^+P$ analysis
- ✓ Interesting avenue to study Fermi motion effects in RG-C data through three particle final state
- ✓ Efforts to test and validate packing fraction/dilution factor for ND_3 , including conversion ratio to analyze all RG-C run periods
- ✓ Preliminary 2D BSA studies results suggest consistency between two and three particle final states, RG-B, $DV\pi^+P$ & preliminary integrated TSA interesting but work remains to clean up results
- Working with RG-C collaborators on troubleshooting and identifying target behaviour issues to progress towards consistent TSA and DSA results across run periods
- Binning for TSA and DSA in 1D, 2D (may not be possible with statistics)
- Three particle final state TSA and DSA studies (may not be possible with statistics)
- Similar systematic studies to RG-C $DV\pi^+P$ analysis



See also:

- T. Hayward, *Exclusive π^+ Spin Asymmetries from RGC and Fermi Motion Smearing Studies* (prev.)
- N. Pilleux, *DVCS on longitudinally polarized protons in deuterium with RGC* (2026/03/12)



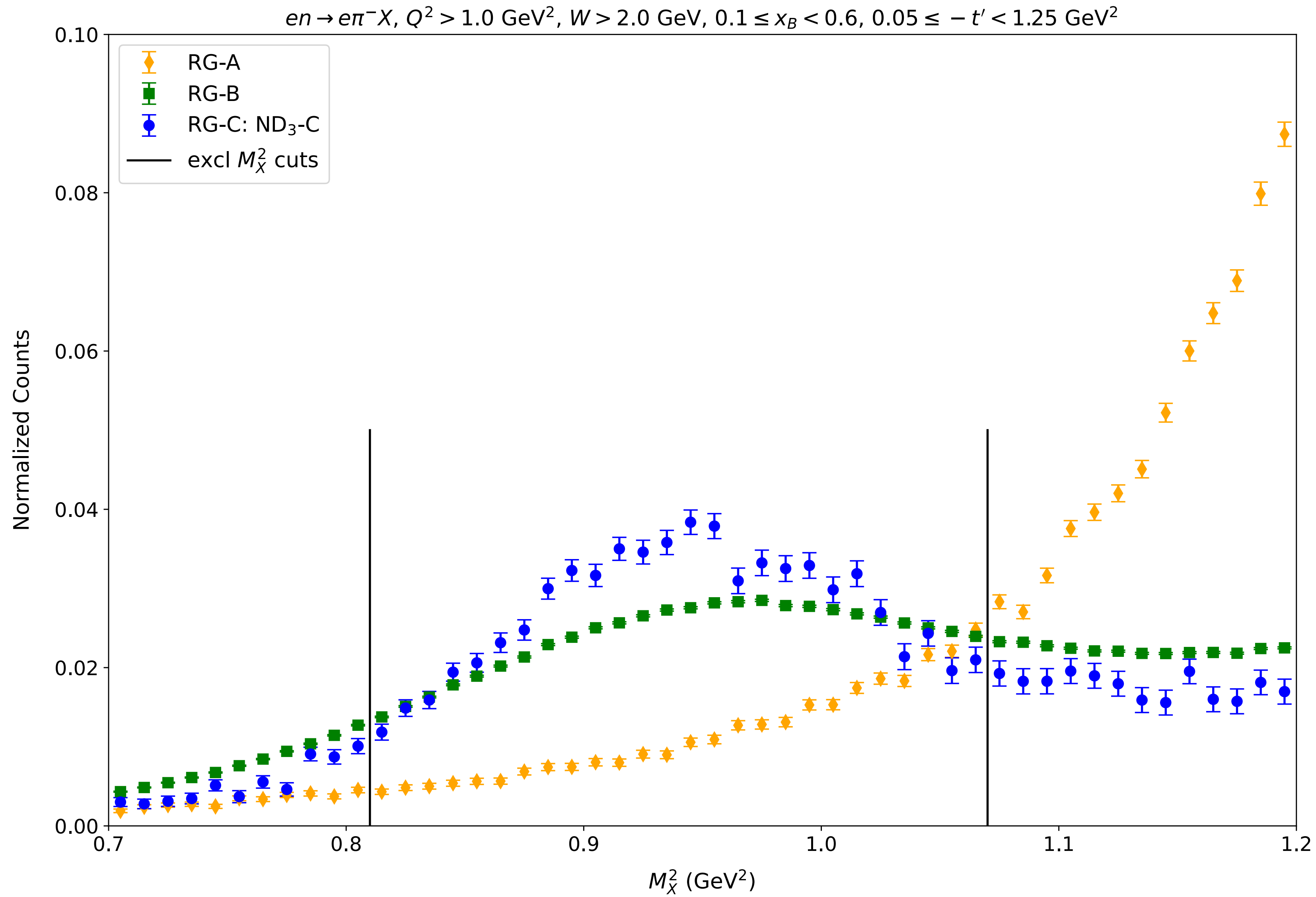
Thank you, questions?



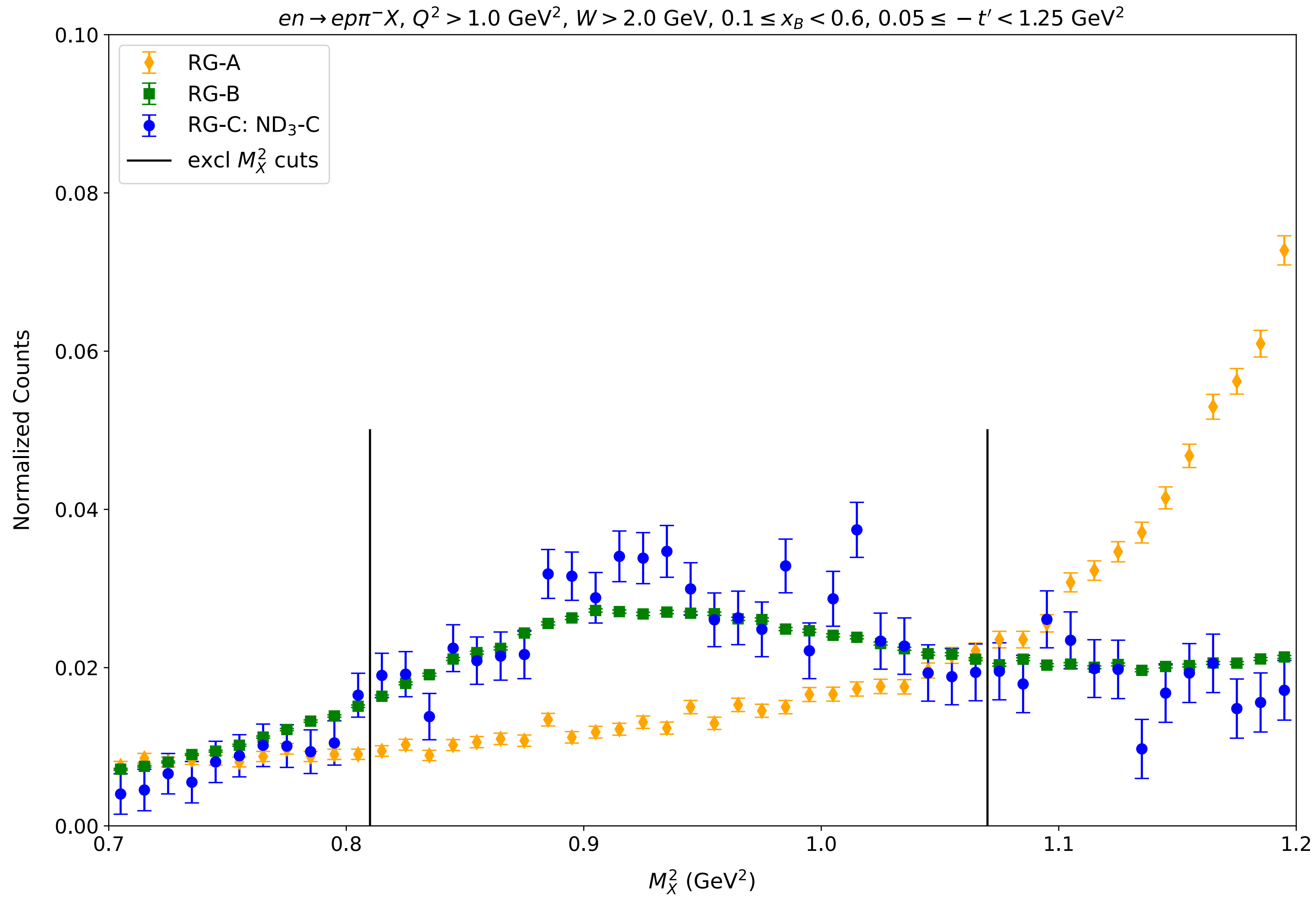
Back-up slides



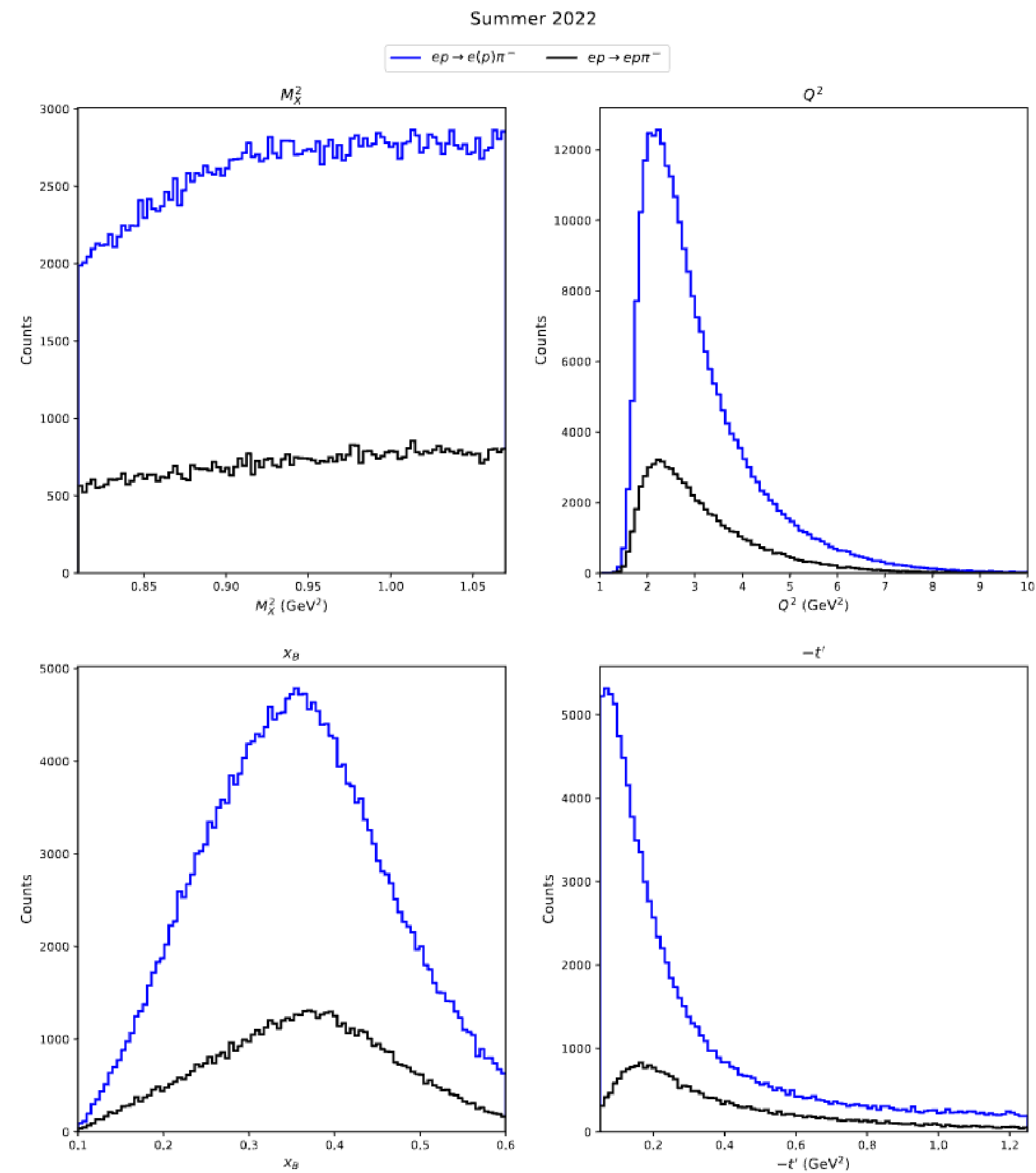
Two particle final state across run periods



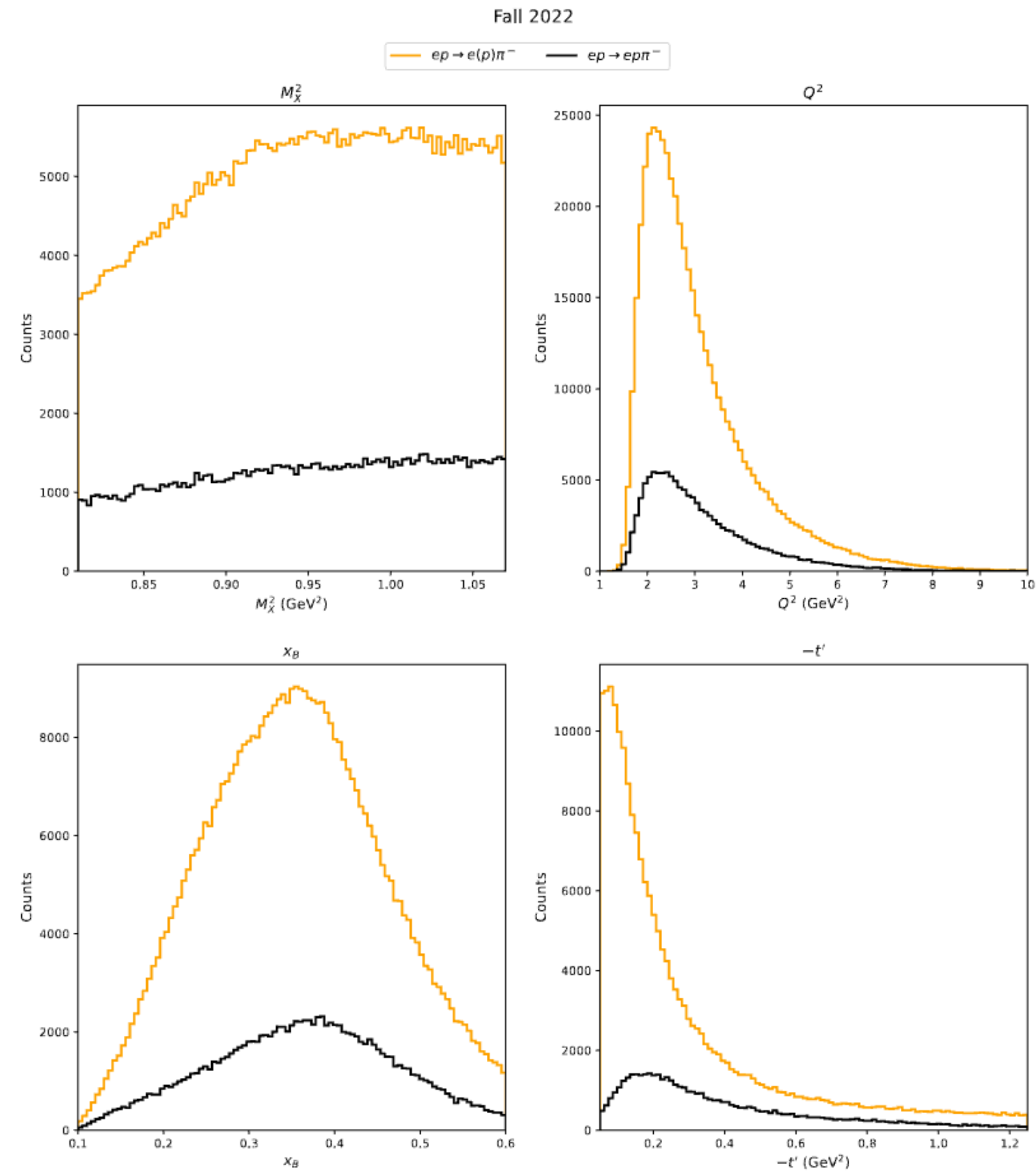
Three particle final state across run periods



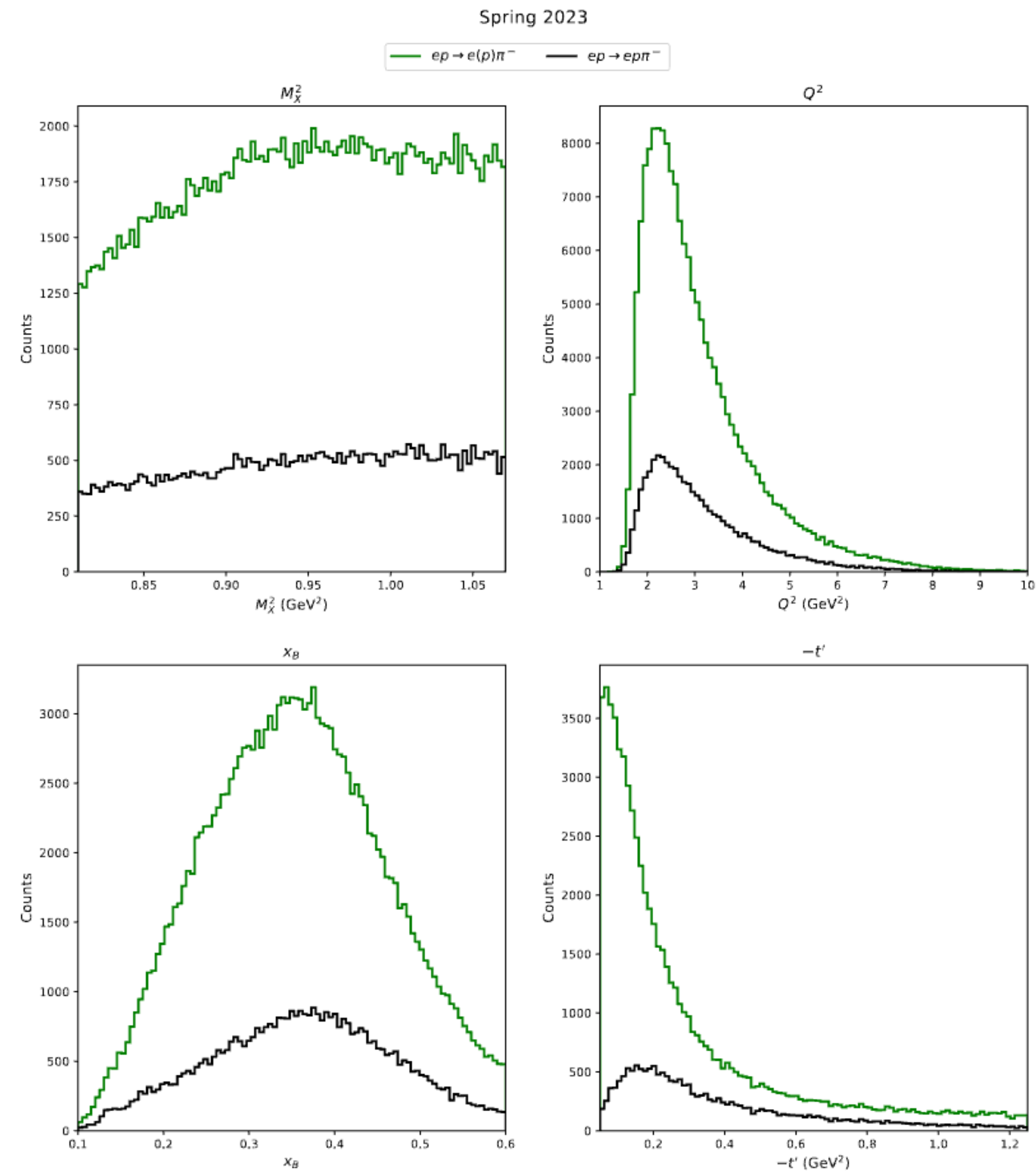
Summer 2022 Yields



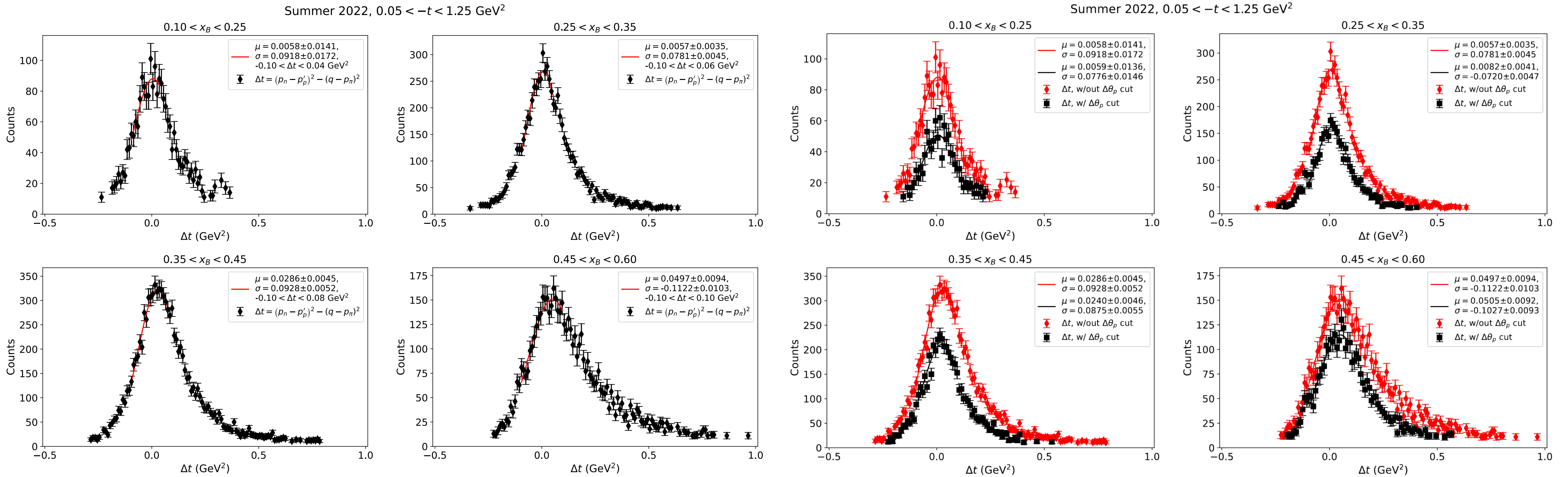
Fall 2022 Yields



Spring 2023 Yields

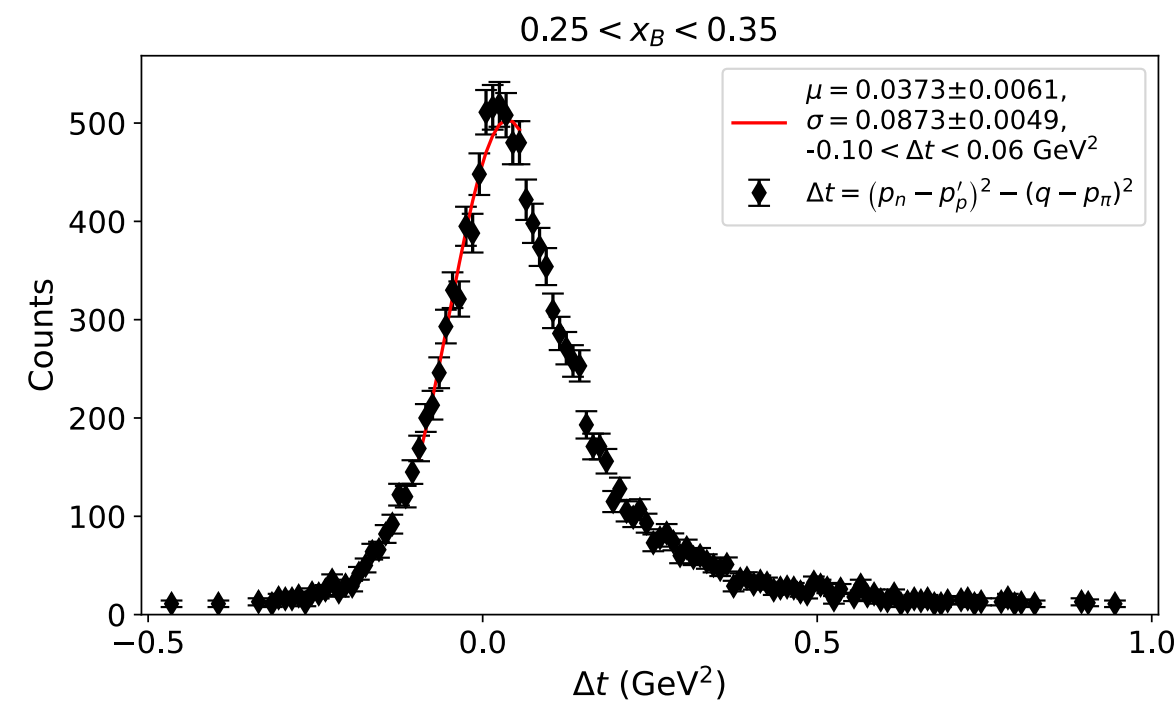
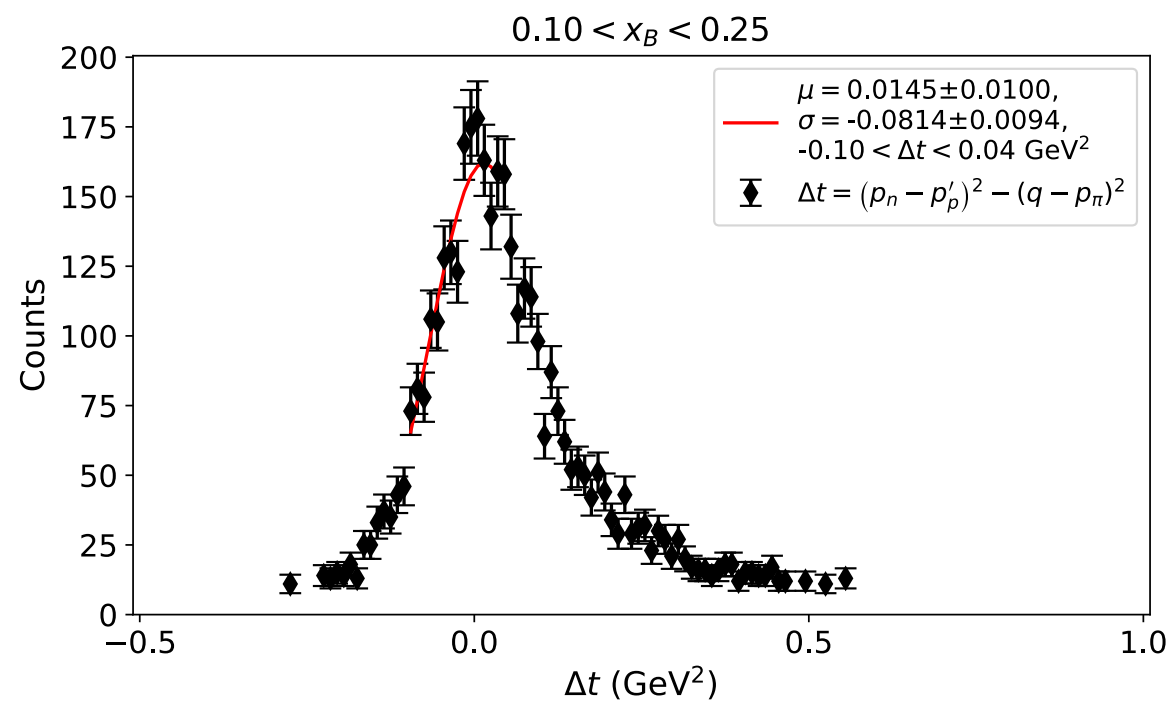


Summer 2022 Δt

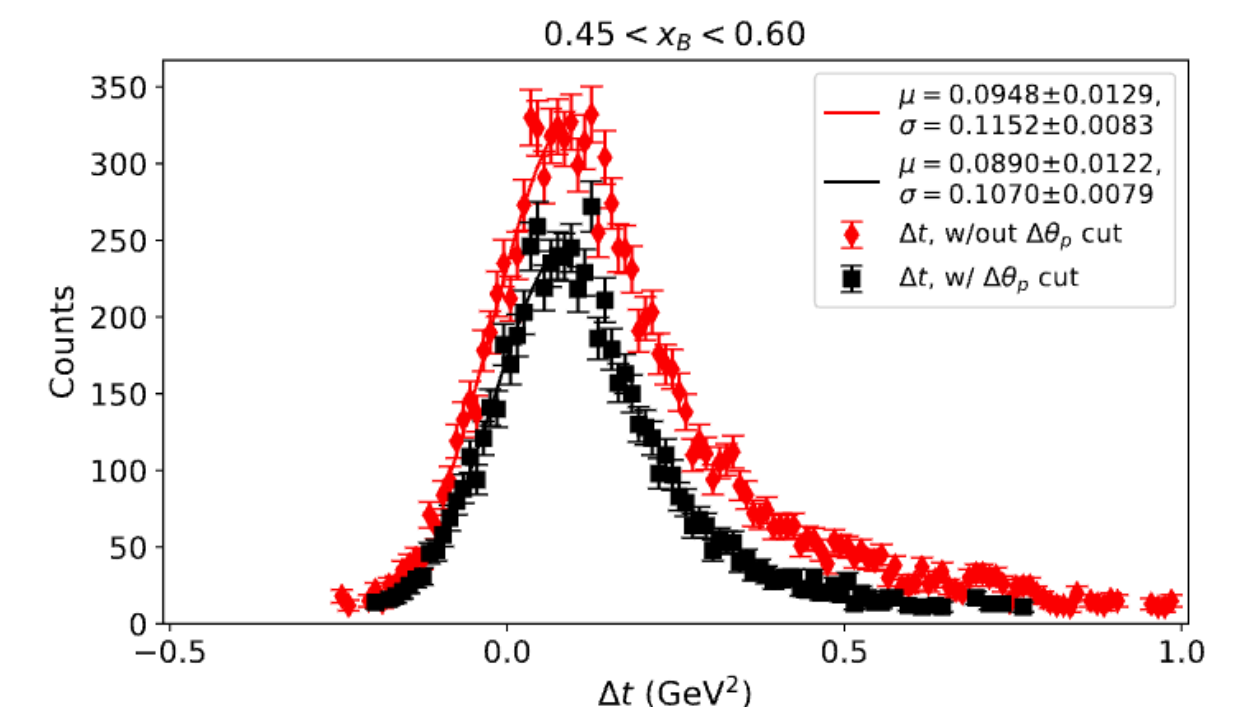
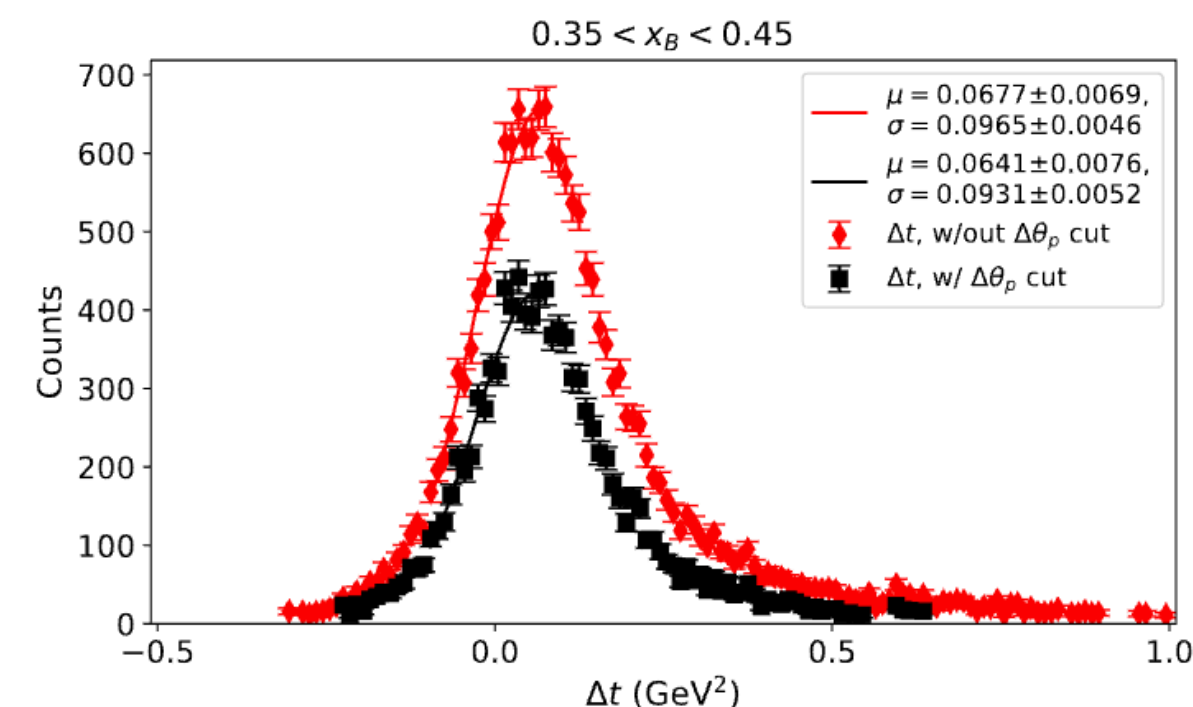
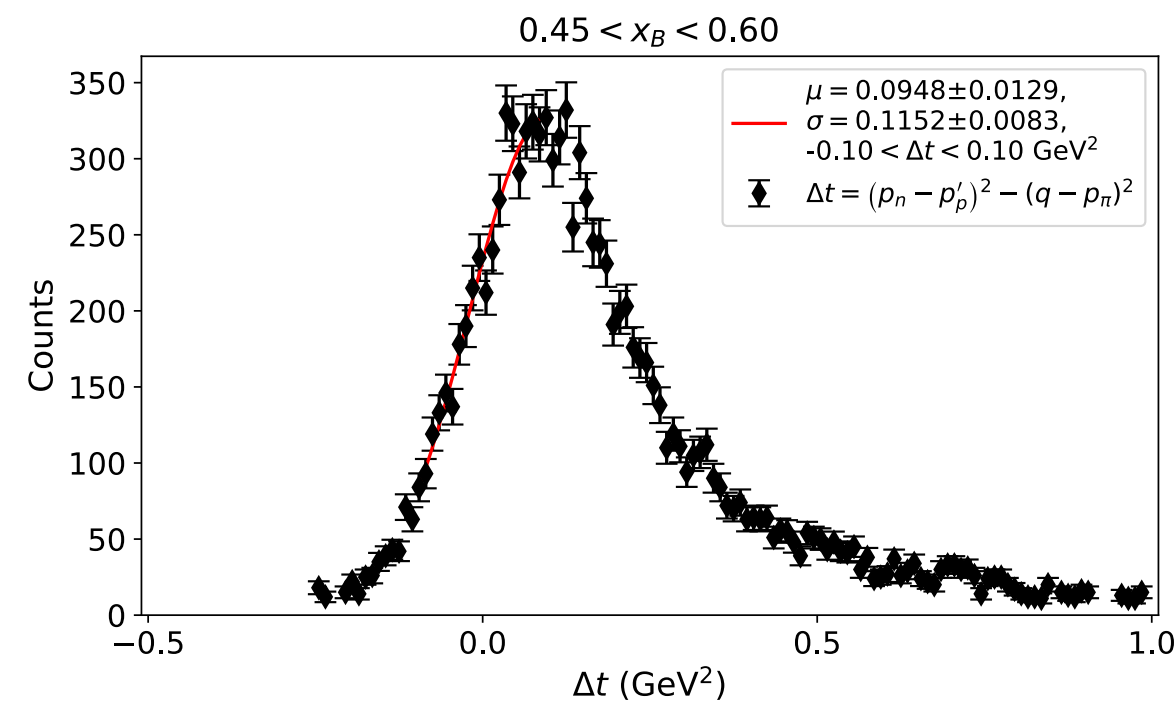
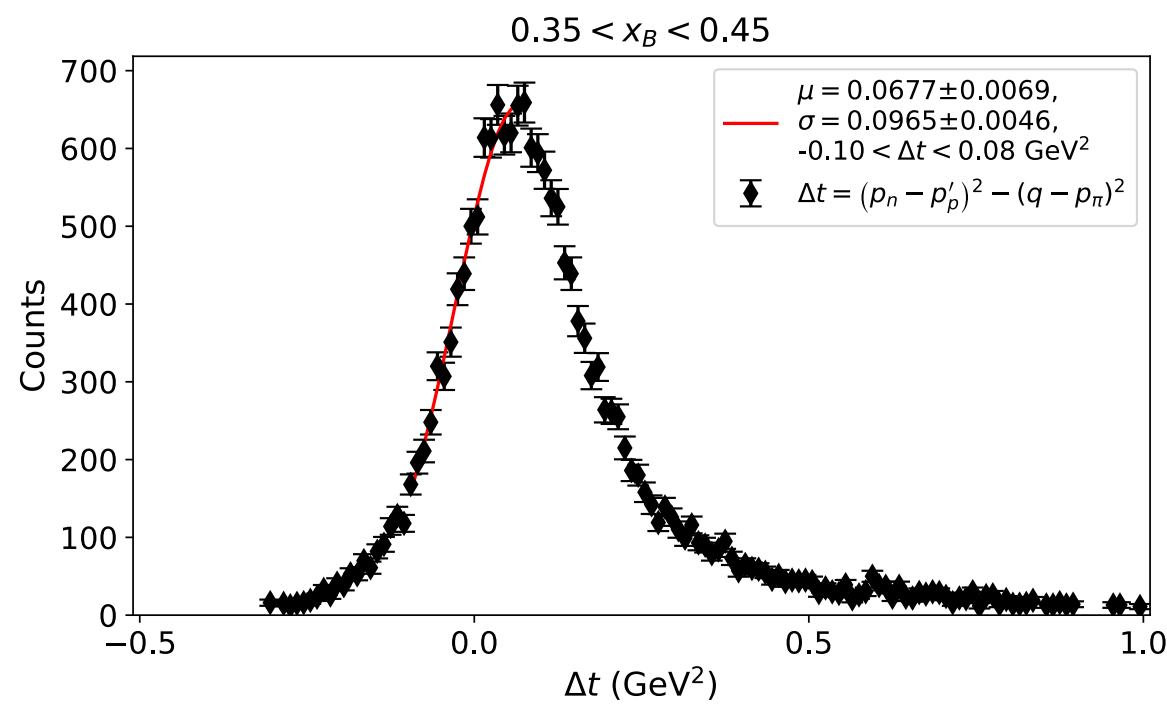
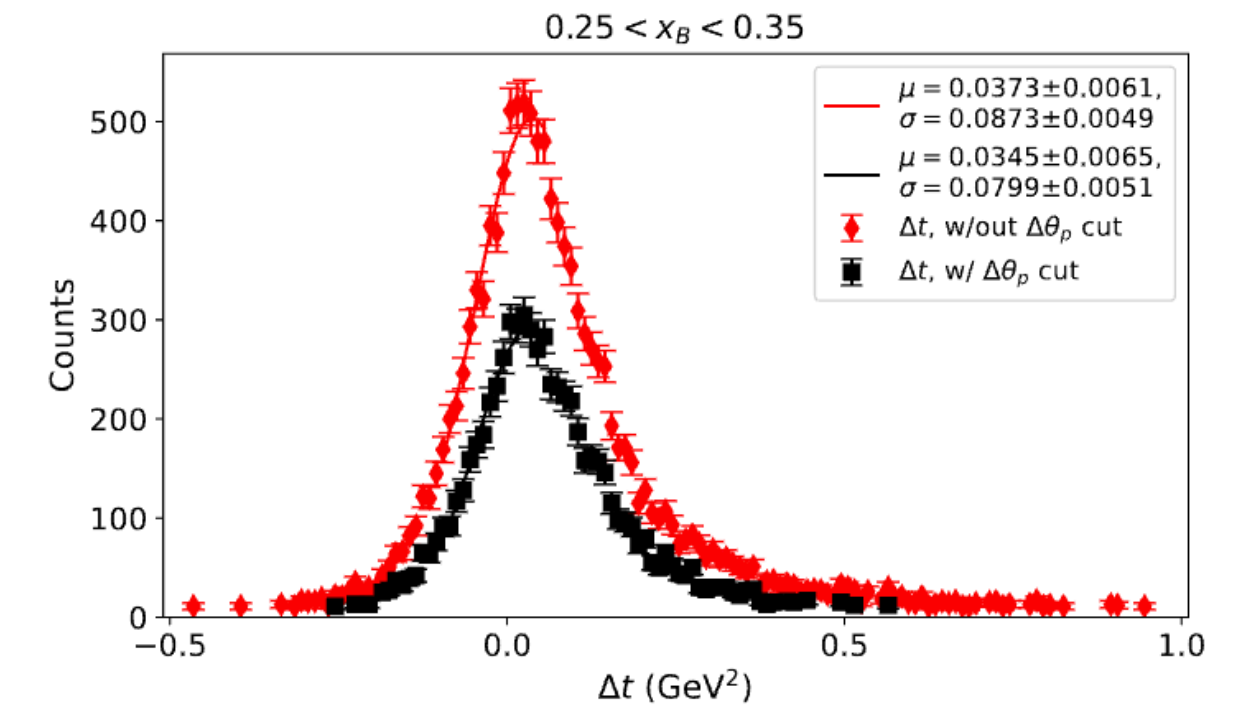
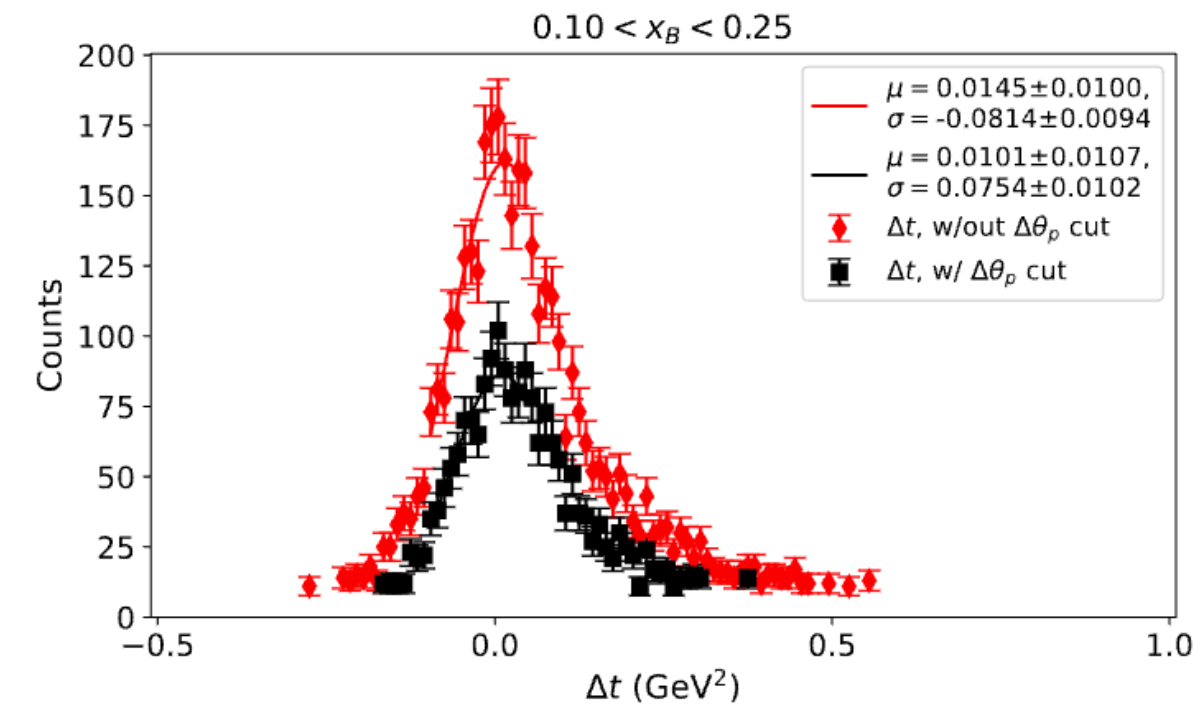


Fall 2022 Δt

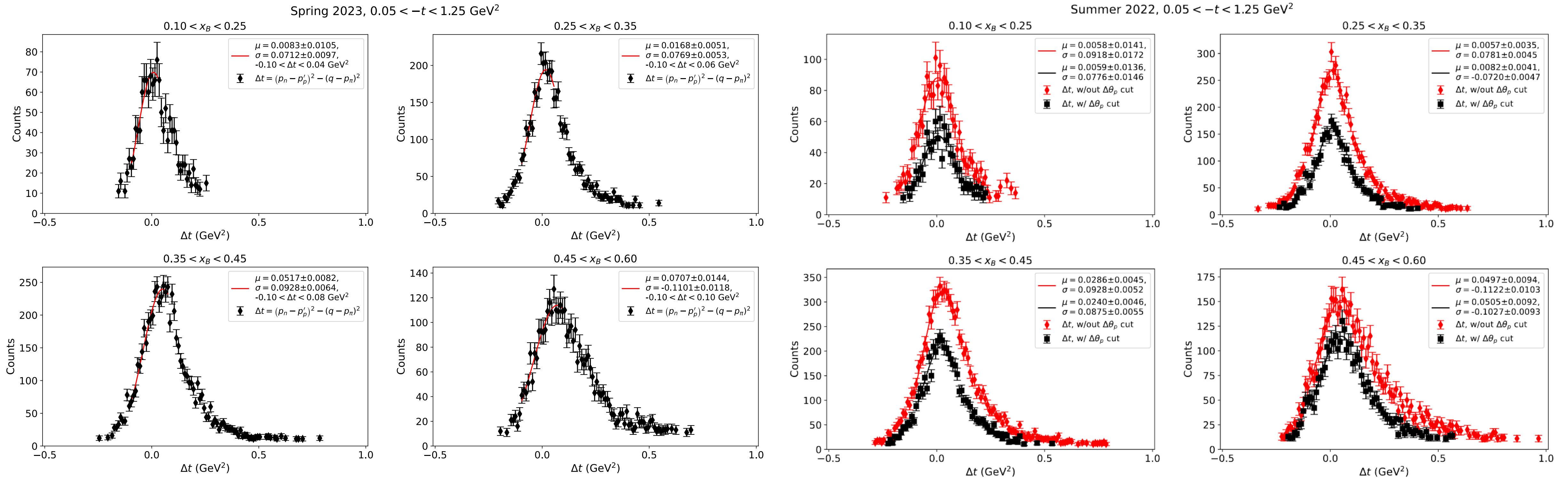
Fall 2022, $0.05 < -t < 1.25 \text{ GeV}^2$



Fall 2022, $0.05 < -t < 1.25 \text{ GeV}^2$



Spring 2023 Δt



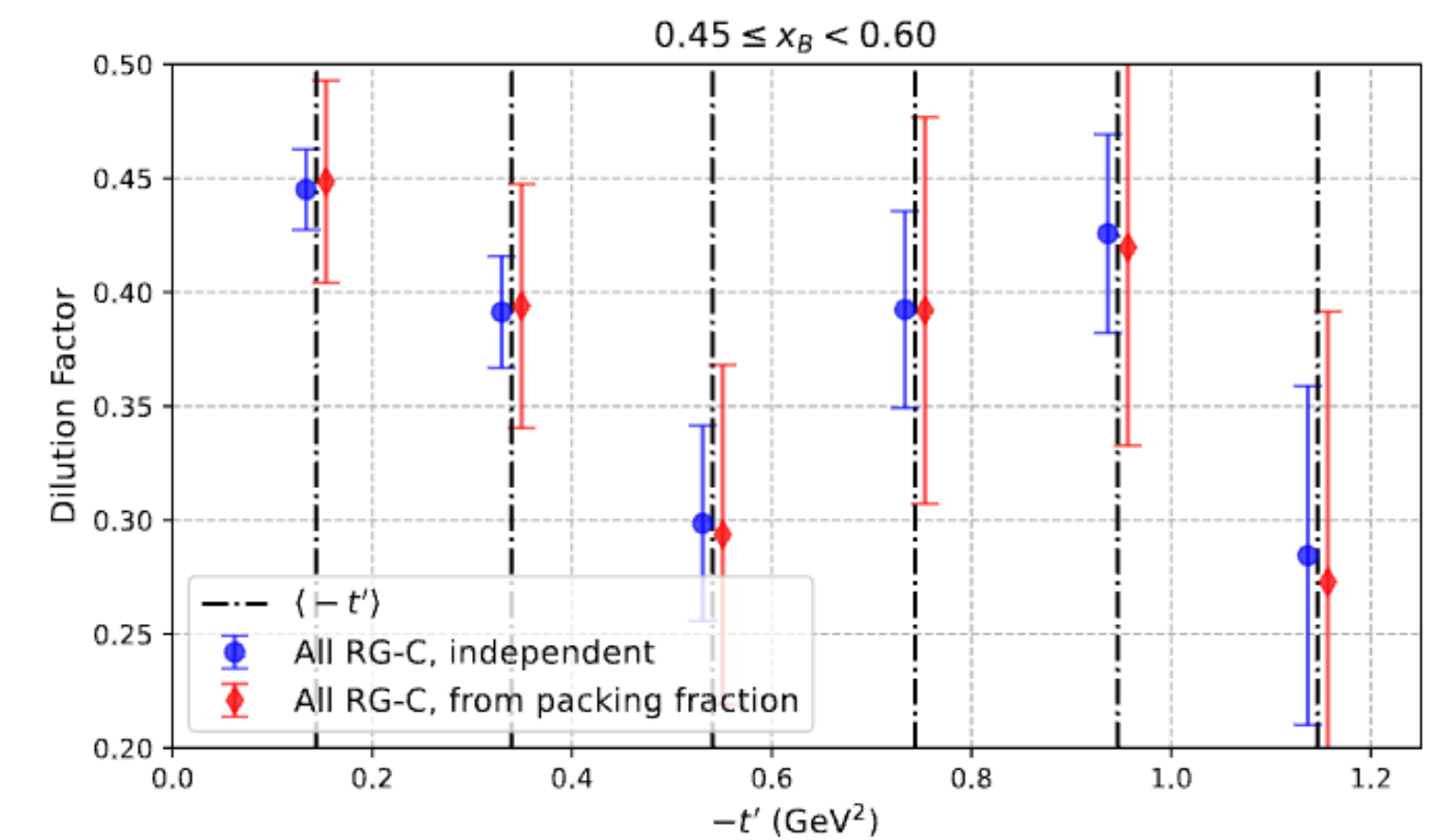
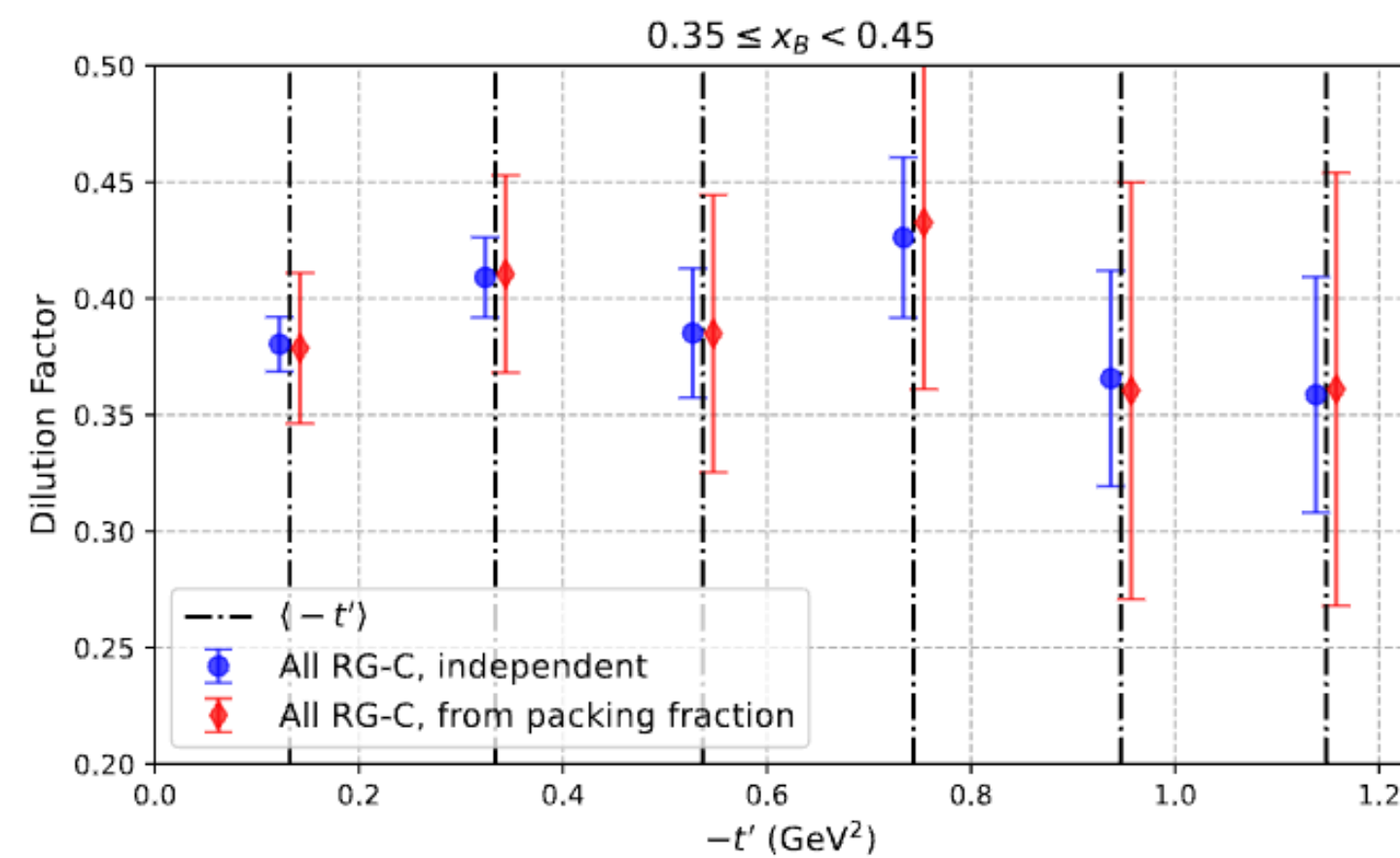
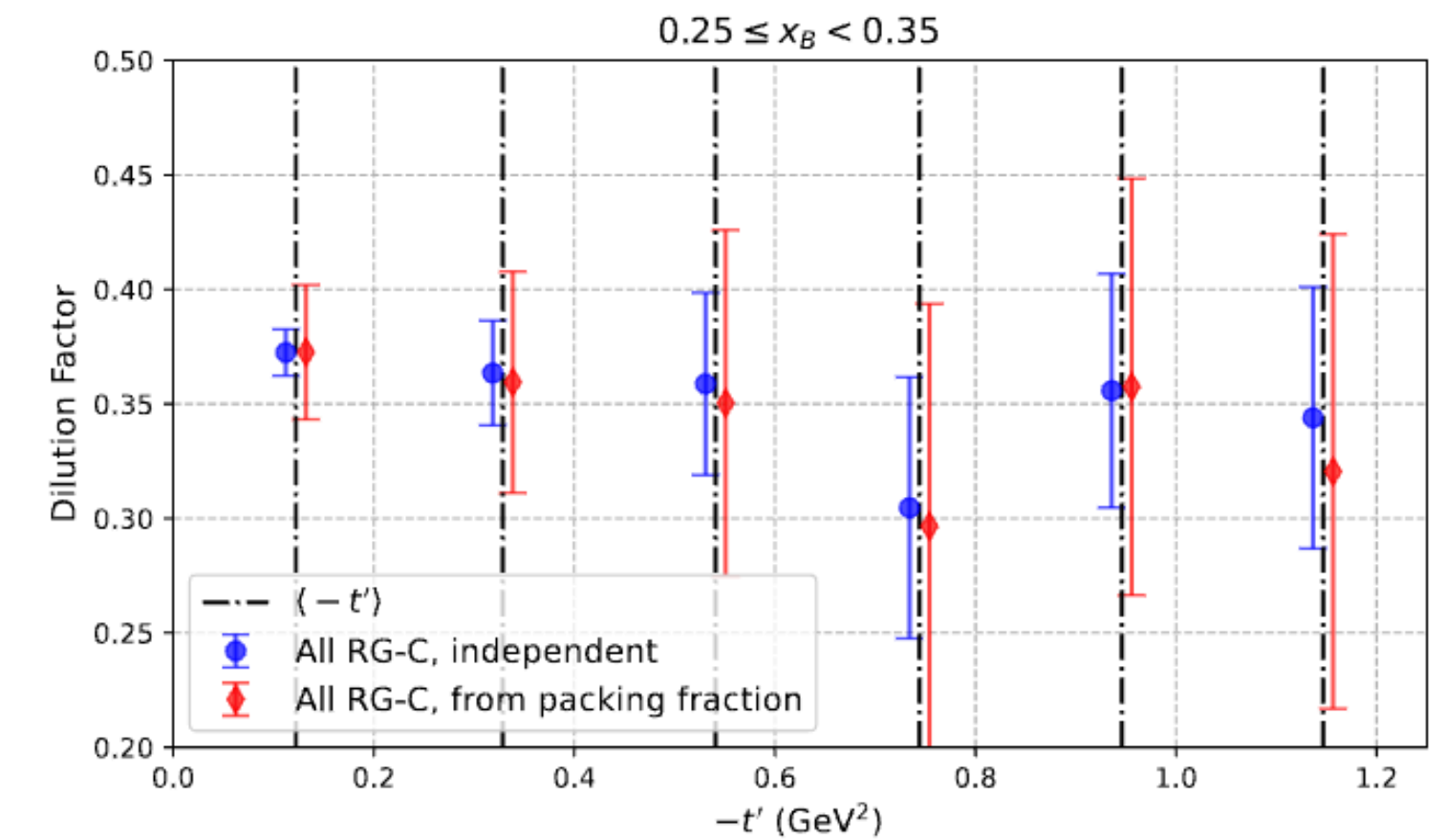
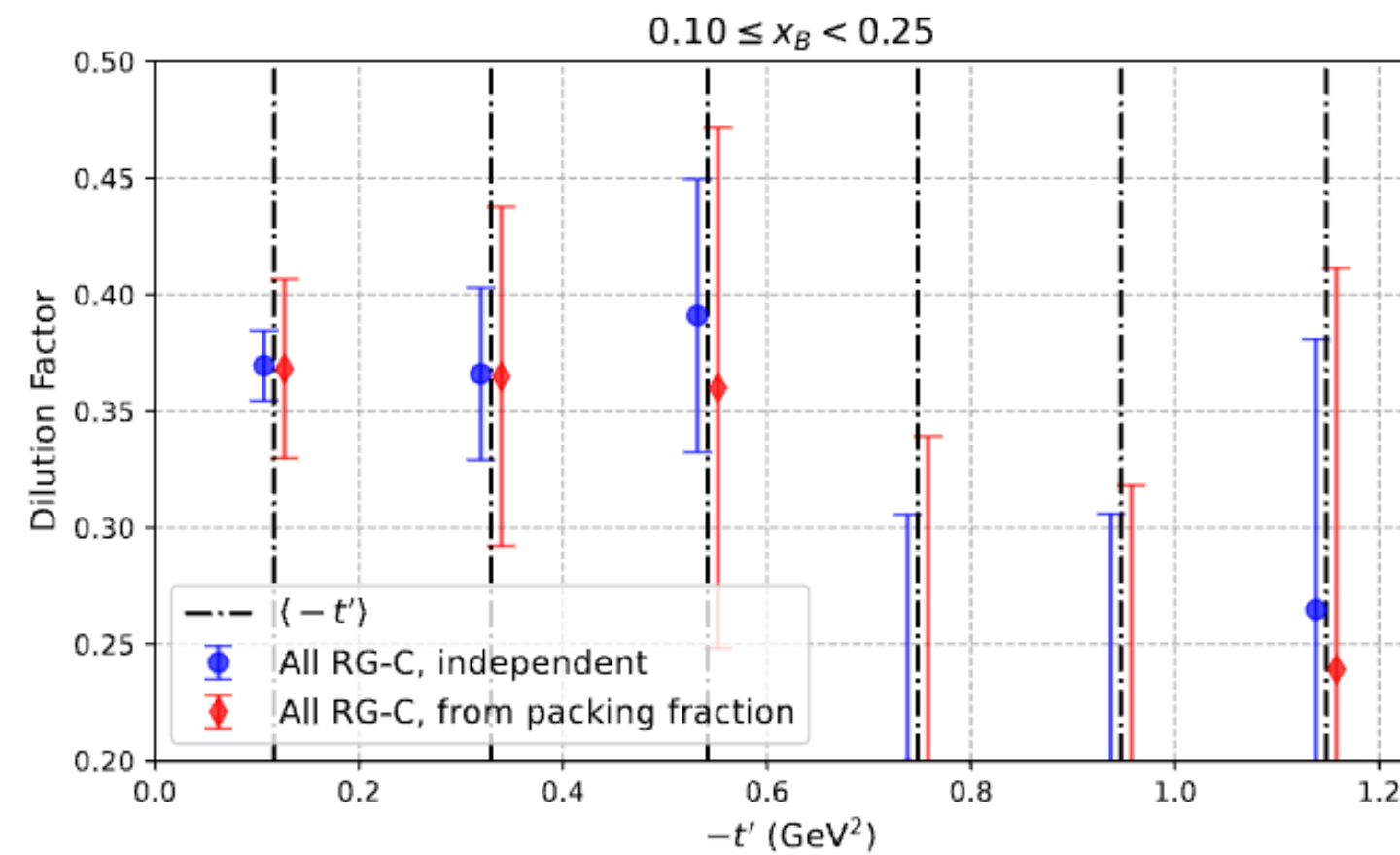
Alternate dilution factor calculation techniques

$$DF = \frac{(n_A - n_{MT})(n_{CD} - 0.757666n_C - 0.005200n_{MT} - 0.237132n_F)}{n_A(n_{CD} - 0.168370n_C - 0.865973n_{MT} + 0.03434n_F)}$$

vs.

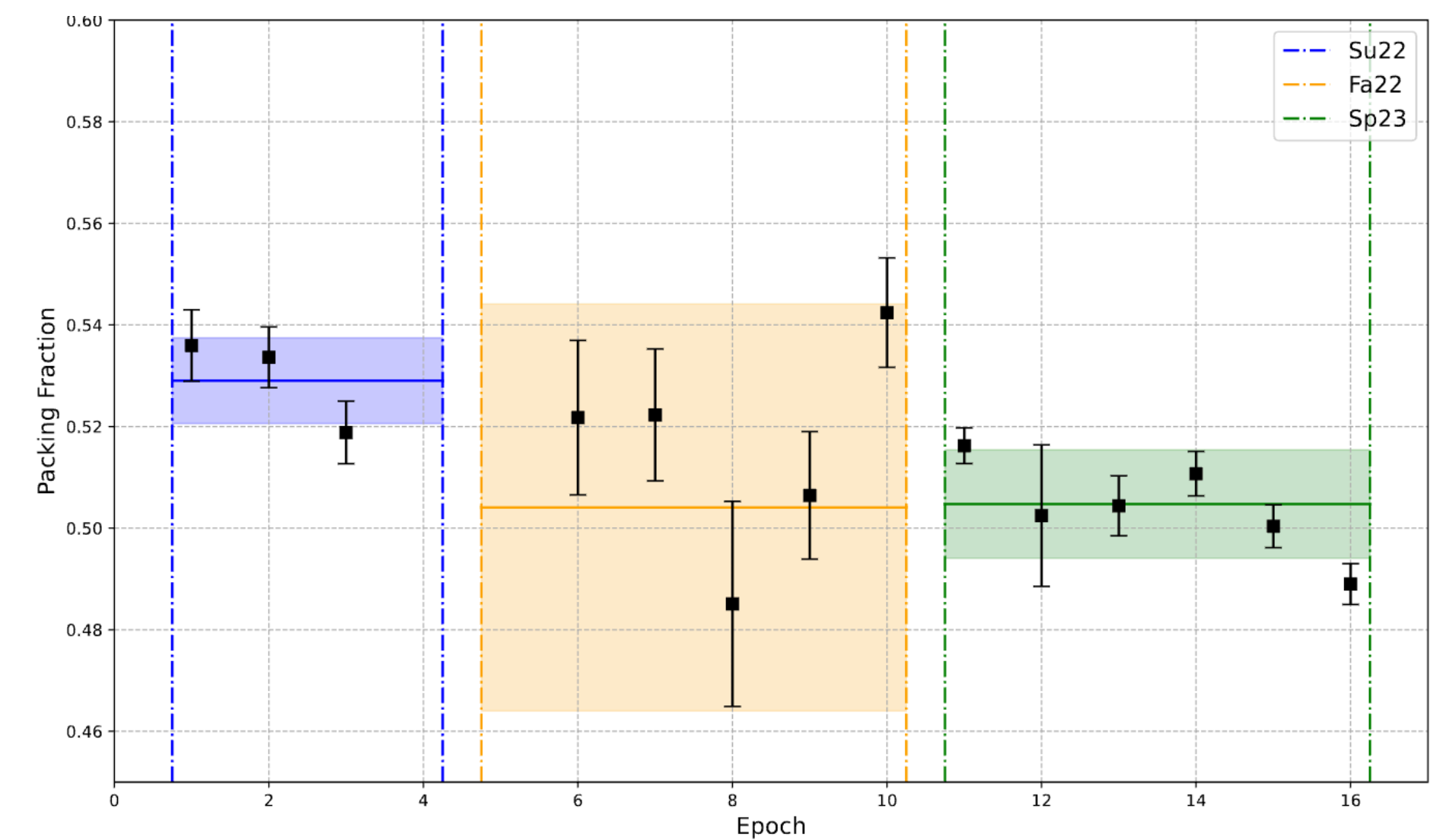
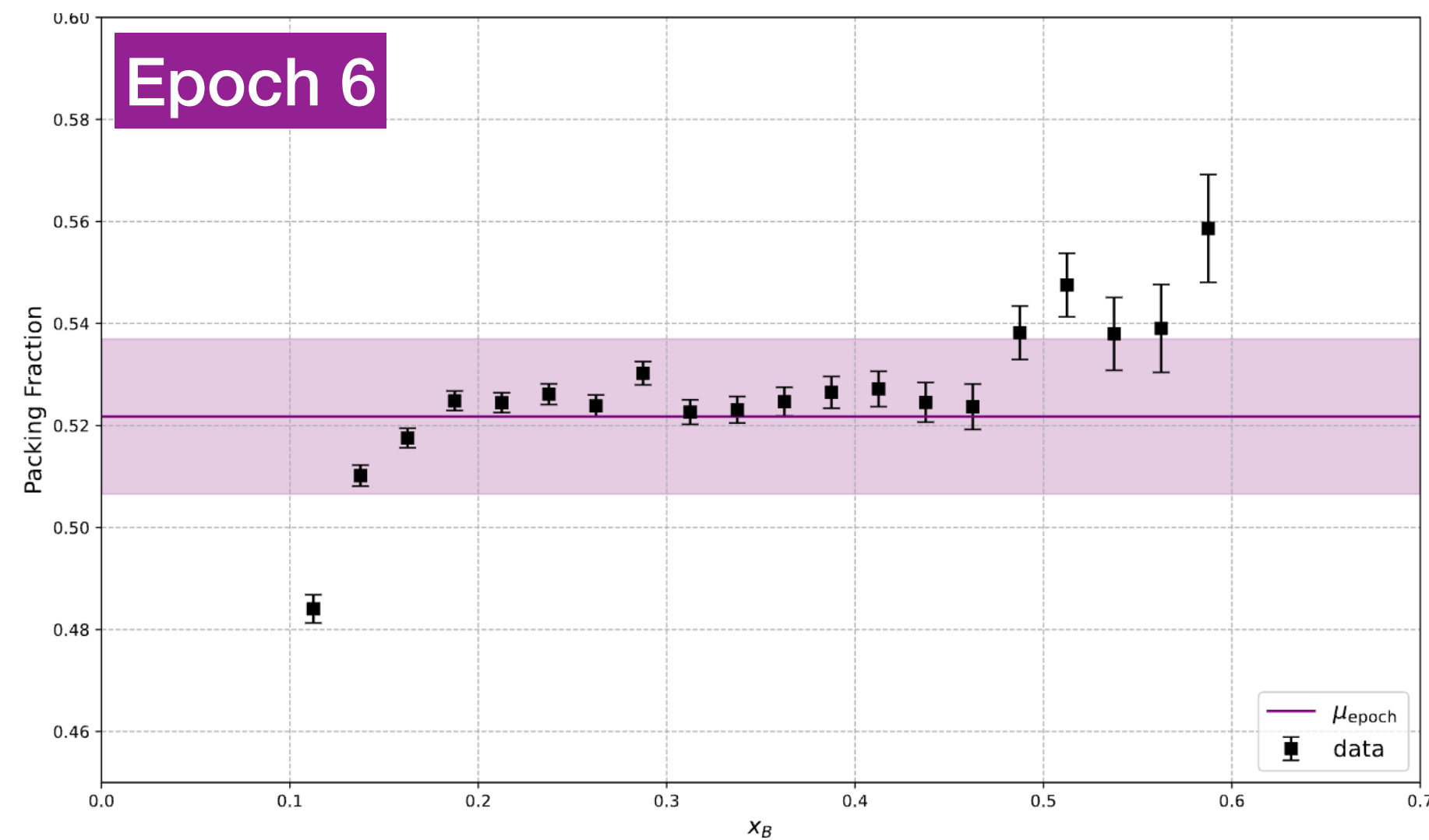
$$DF = 2.260129 \frac{PF}{n_A} (n_{CD} - 0.757666n_C - 0.005200n_{MT} - 0.237132n_F)$$

shown for $en \rightarrow e(p)\pi^-$



Packing fraction studies

Also useful to extract packing fraction of each run period epoch to measure consistency, shown here without M_X^2 cuts for larger sample size



Individual epoch, $Pf(x_B)$

Averages across all epochs in run-period



→ Still a work in progress to get perfect agreement in epoch packing fraction results across run group, but in general consistent to order of ~5%



Asymmetry observables → structure functions

$$A_{LU} = C_{LU} + \frac{\frac{W}{A} A_{LU}^{\sin \phi} \sin \phi}{1 + \frac{V}{A} A_{UU}^{\cos \phi} \cos \phi + \frac{B}{A} A_{UU}^{\cos 2\phi} \cos 2\phi} = \frac{1}{P_b} \frac{P_t^- (n^{++} - n^{-+}) + P_t^+ (n^{+-} - n^{--})}{P_t^- (n^{++} + n^{-+}) + P_t^+ (n^{+-} + n^{--})}$$

$$A_{UL} = C_{UL} + \frac{\frac{V}{A} A_{UL}^{\sin \phi} \sin \phi + \frac{B}{A} A_{UL}^{\sin 2\phi} \sin 2\phi}{1 + \frac{V}{A} A_{UU}^{\cos \phi} \cos \phi + \frac{B}{A} A_{UU}^{\cos 2\phi} \cos 2\phi} = \frac{1}{D_f} \frac{(n^{++} + n^{-+}) - (n^{+-} + n^{--})}{P_t^- (n^{++} + n^{-+}) + P_t^+ (n^{+-} + n^{--})}$$

$$A_{LL} = \frac{\frac{C}{A} A_{LL}^{\cos 0\phi} + \frac{W}{A} A_{LL}^{\cos \phi} \cos \phi}{1 + \frac{V}{A} A_{UU}^{\cos \phi} \cos \phi + \frac{B}{A} A_{UU}^{\cos 2\phi} \cos 2\phi} = \frac{1}{P_b D_f} \frac{(n^{++} - n^{-+}) + (-n^{+-} + n^{--})}{P_t^- (n^{++} + n^{-+}) + P_t^+ (n^{+-} + n^{--})}$$

$$n^{bt} = \frac{N^{bt}}{F_{CC}^{bt}}$$

simultaneous fit to extract consistent structure functions

+ transversely polarized photon contributions to A_{UL}, A_{LL}

A, B, C, V, W depolarization factors →

$$A(\epsilon, y) \equiv \frac{y^2}{2(1-\epsilon)} = \frac{1}{1+\gamma^2} \left(1 - y + \frac{1}{2}y^2 + \frac{1}{4}\gamma^2 y^2 \right) \approx \left(1 - y + \frac{1}{2}y^2 \right),$$

$$B(\epsilon, y) \equiv \frac{y^2}{2(1-\epsilon)} \epsilon = \frac{1}{1+\gamma^2} \left(1 - y - \frac{1}{4}\gamma^2 y^2 \right) \approx (1 - y),$$

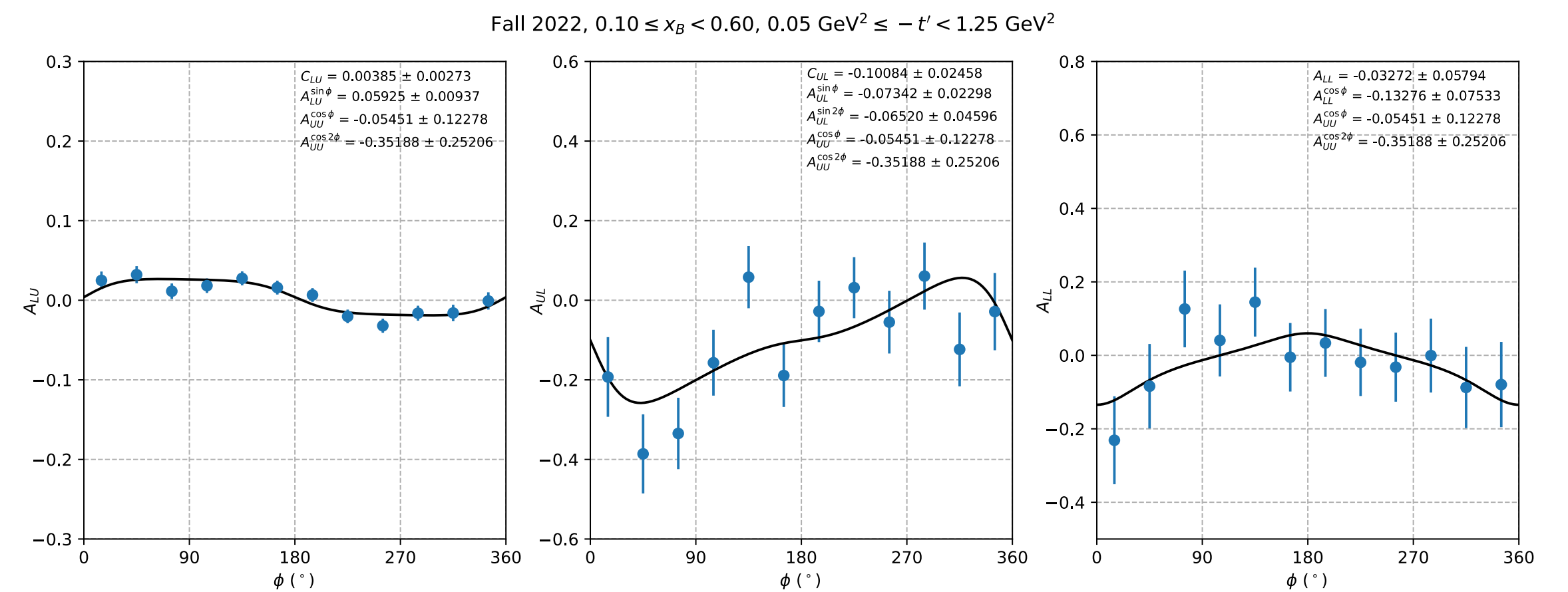
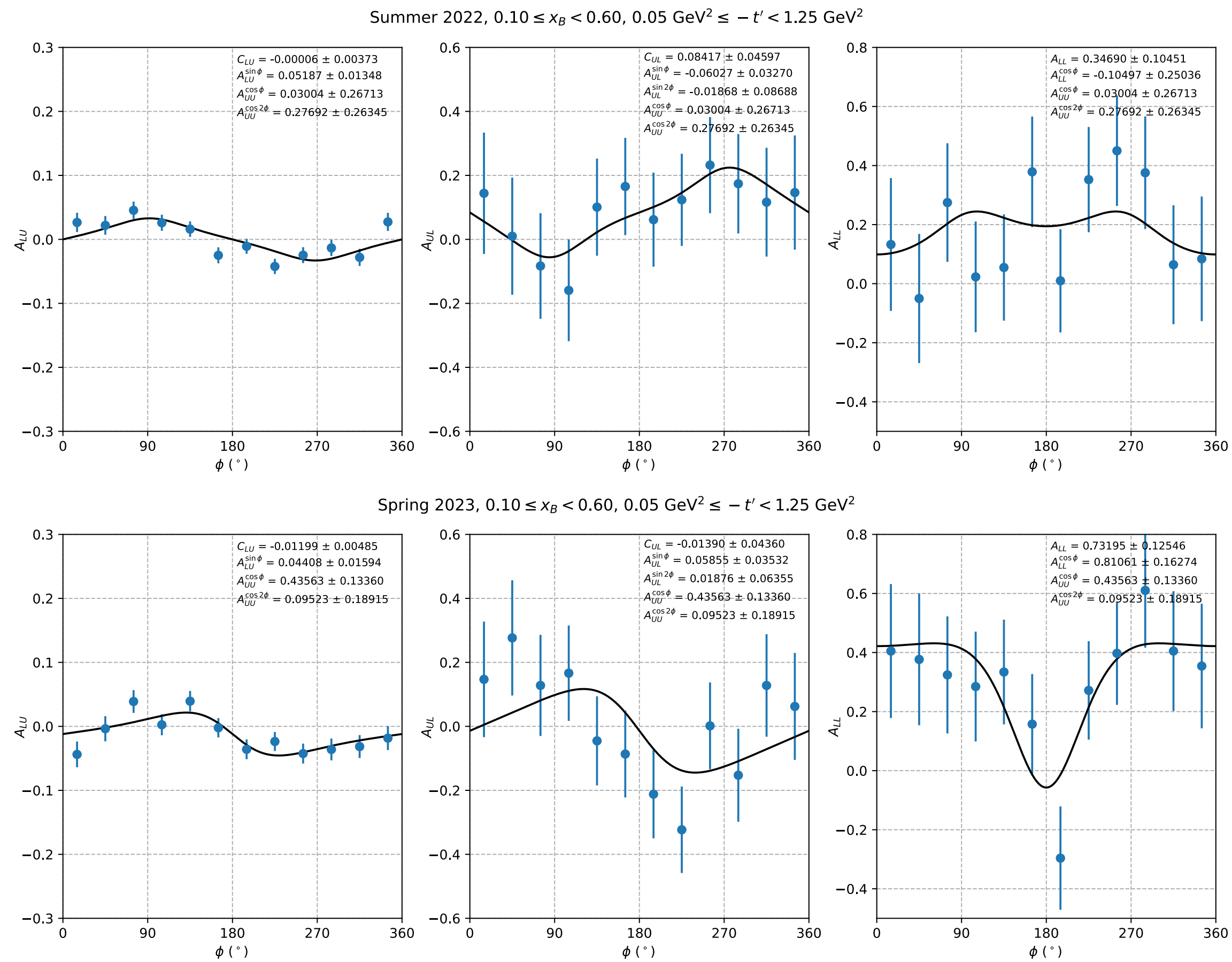
$$C(\epsilon, y) \equiv \frac{y^2}{2(1-\epsilon)} \sqrt{1-\epsilon^2} = \frac{y}{\sqrt{1+\gamma^2}} \left(1 - \frac{1}{2}y \right) \approx y \left(1 - \frac{1}{2}y \right),$$

$$V(\epsilon, y) \equiv \frac{y^2}{2(1-\epsilon)} \sqrt{2\epsilon(1+\epsilon)} = \frac{2-y}{1+\gamma^2} \sqrt{1-y - \frac{1}{4}\gamma^2 y^2} \approx (2-y) \sqrt{1-y},$$

$$W(\epsilon, y) \equiv \frac{y^2}{2(1-\epsilon)} \sqrt{2\epsilon(1-\epsilon)} = \frac{y}{\sqrt{1+\gamma^2}} \sqrt{1-y - \frac{1}{4}\gamma^2 y^2} \approx y \sqrt{1-y},$$

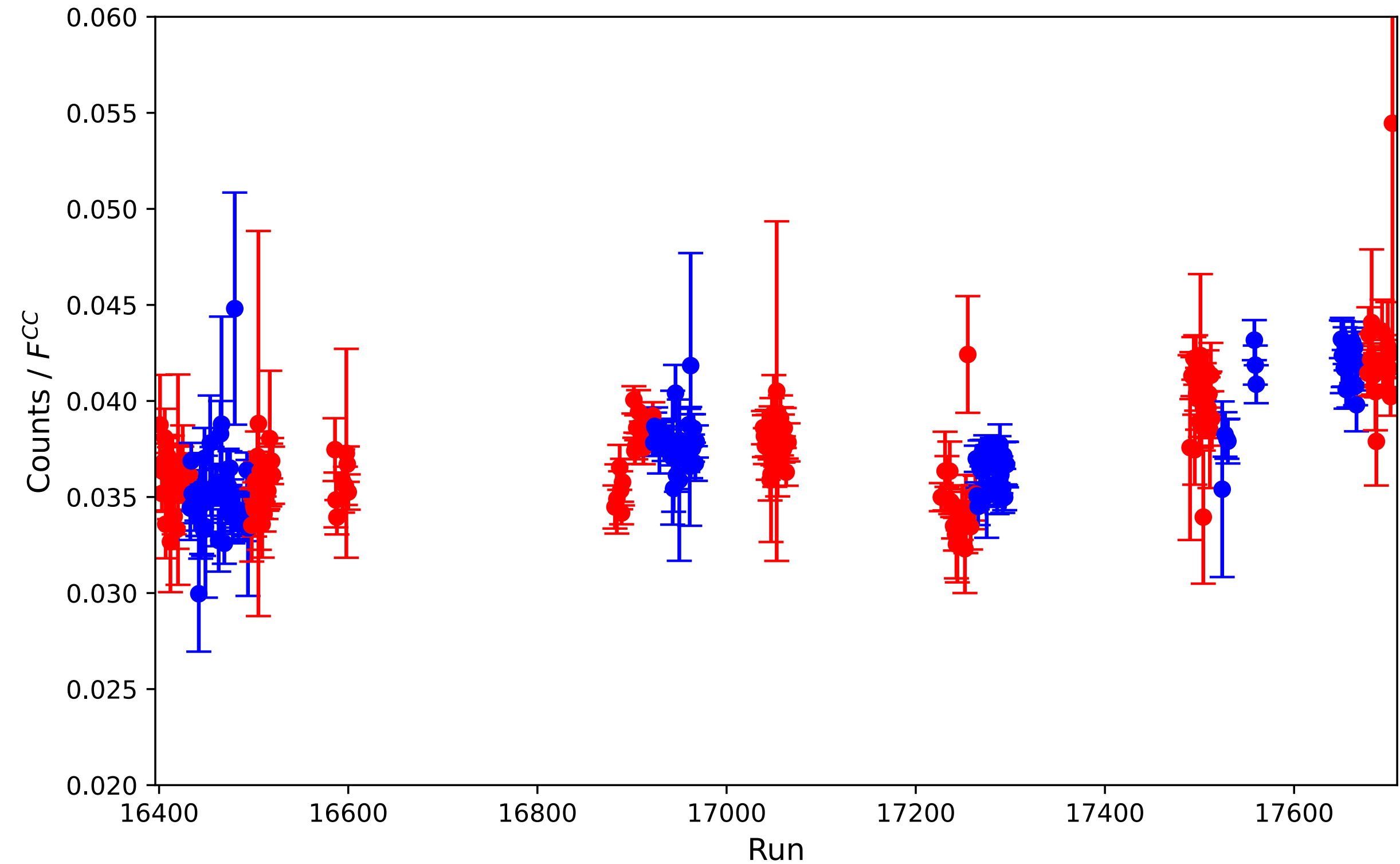
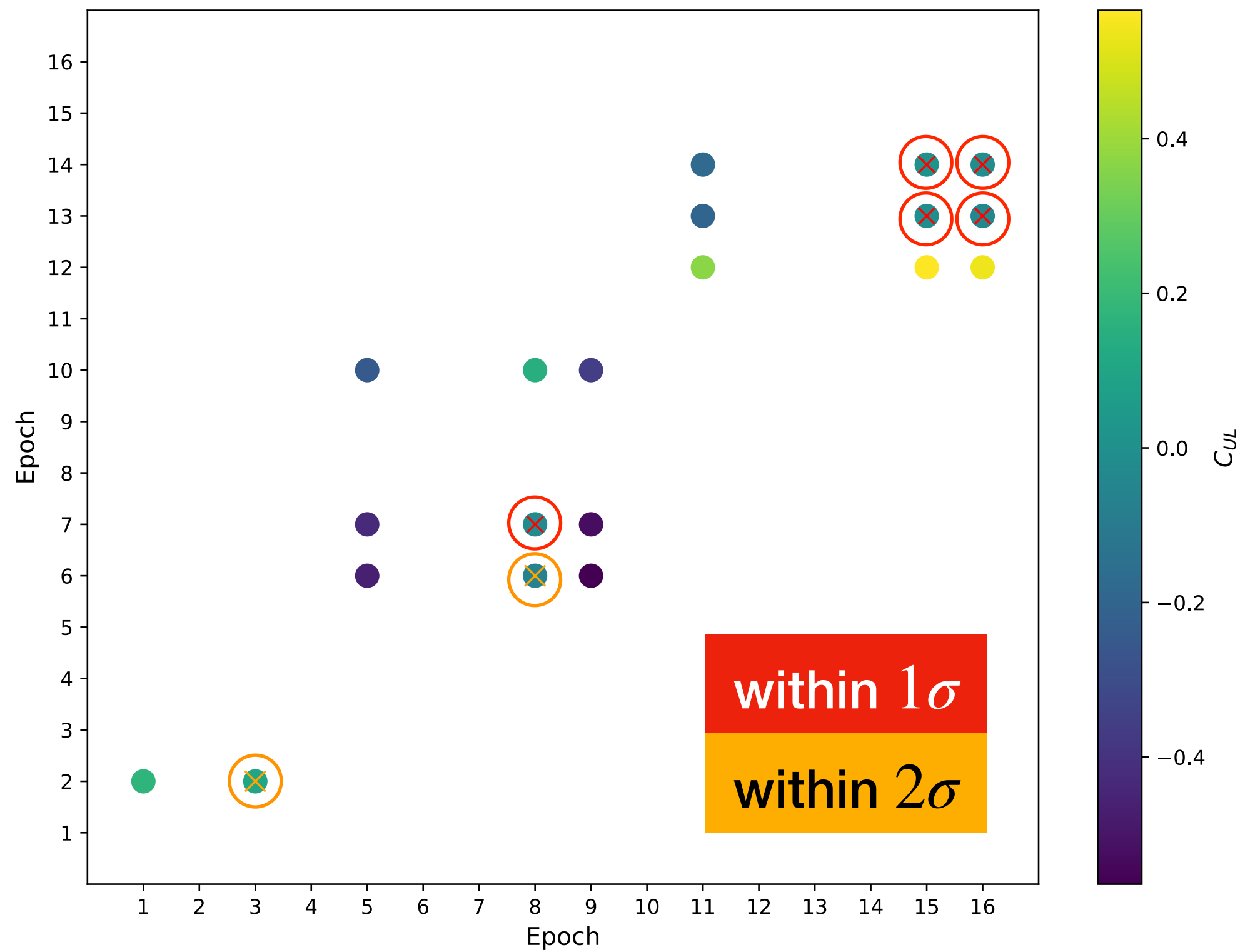


(Very) preliminary spin asymmetry set results across all run periods



Troubleshooting target spin asymmetry

C_{UL} consistency per epoch



Positive target polarization

Negative target polarization



Some examples of what we've been working on...

